Stem Cell Reports
Article
OPEN ACCESS

Cellular Adjuvant Properties, Direct Cytotoxicity of Re-differentiated Vα24 Invariant NKT-like Cells from Human Induced Pluripotent Stem Cells

Shuichi Kitayama,[1,7] Rong Zhang,[2,6,7] Tian-Yi Liu,[2,3] Norihiro Ueda,[1,2] Shoichi Iriguchi,[1] Yutaka Yasui,[1] Yohei Kawai,[1] Minako Tatsumi,[2] Norihito Hirai,[1] Yasutaka Mizoro,[4] Tatsuaki Iwama,[6] Akira Watanabe,[4] Mahito Nakanishi,[5] Kiyotaka Kuzushima,[2] Yasushi Uemura,[2,6,8,*] and Shin Kaneko[1,8,*]

[1]Shin Kaneko Laboratory, Department of Cell Growth and Differentiation, Center for iPS Cell Research and Application (CiRA), Kyoto University, 53 Shogoin Kawahara-cho, Sakyo-ku, Kyoto 606-8501, Japan
[2]Division of Immunology, Aichi Cancer Center Research Institute (ACCRI), 1-1 Kanokoden, Chikusa-ku, Nagoya, Aichi 464-8681, Japan
[3]Key Laboratory of Cancer Center, Chinese PLA General Hospital, 28 Fuxing Road, Beijing 100853, China
[4]Sequencing Core Facility, CiRA, Kyoto University, 53 Shogoin Kawahara-cho, Sakyo-ku, Kyoto 606-8501, Japan
[5]Research Center for Stem Cell Engineering, National Institute of Advanced Industrial Science and Technology (AIST), 1-1-1 Higashi, Tsukuba, Ibaraki 305-8561, Japan
[6]Division of Cancer Immunotherapy, Exploratory Oncology Research & Clinical Trial Center, National Cancer Center (NCC), 6-5-1 Kashiwanoha, Kashiwa, Chiba 277-8577, Japan
[7]Co-first author
[8]Co-senior author
*Correspondence: yuemura@east.ncc.go.jp (Y.U.), kaneko.shin@cira.kyoto-u.ac.jp (S.K.)
http://dx.doi.org/10.1016/j.stemcr.2016.01.005

SUMMARY

Vα24 invariant natural killer T (iNKT) cells are a subset of T lymphocytes implicated in the regulation of broad immune responses. They recognize lipid antigens presented by CD1d on antigen-presenting cells and induce both innate and adaptive immune responses, which enhance effective immunity against cancer. Conversely, reduced iNKT cell numbers and function have been observed in many patients with cancer. To recover these numbers, we reprogrammed human iNKT cells to pluripotency and then re-differentiated them into regenerated iNKT cells in vitro through an IL-7/IL-15-based optimized cytokine combination. The re-differentiated iNKT cells showed proliferation and IFN-γ production in response to α-galactosylceramide, induced dendritic cell maturation and downstream activation of both cytotoxic T lymphocytes and NK cells, and exhibited NKG2D- and DNAM-1-mediated NK cell-like cytotoxicity against cancer cell lines. The immunological features of re-differentiated iNKT cells and their unlimited availability from induced pluripotent stem cells offer a potentially effective immunotherapy against cancer.

INTRODUCTION

Cytotoxic T lymphocytes (CTLs) play a crucial role in the eradication of cancer cells by precisely recognizing them via tumor antigen-specific T cell receptors (TCRs) in a peptide-dependent, human leukocyte antigen (HLA)-restricted manner (Maus et al., 2014). Sometimes, however, cancer cells can proliferate due to absent or dysfunctional CTLs, thus creating demand for immunotherapies. We and another group recently reported the unlimited production of target antigen-specific human $CD8^+$ T lymphocytes from induced pluripotent stem cells (iPSCs) (Nishimura et al., 2013; Vizcardo et al., 2013). This technology has the potential to overcome two important problems currently facing T cell immunotherapies: a shortage of tumor antigen-specific T cells and their exhaustion induced by continuous TCR stimulation and overproliferation (Schietinger and Greenberg, 2014). However, other problems in T cell immunotherapies must also be overcome. One example is the emergence of tumor escape from antigen-specific monoclonal CTLs due to tumor immune-editing involving tumor antigen mutagenesis or HLA depression (Schreiber et al., 2011). Another problem is local immunosuppression in the tumor microenvironment by instigated immune cells, which supports tumor growth and inhibits CTL activities (Mittal et al., 2014; Motz and Coukos, 2013; Noy and Pollard, 2014). A good approach to overcome these problems would be combination therapy using a cellular adjuvant, i.e., invariant natural killer T (iNKT) cells, as iNKT cells exert helper functions to induce antigen-specific polyclonal CTLs (Cerundolo et al., 2009), improve the immunosuppressive milieu (De Santo et al., 2010), and maintain memory $CD8^+$ T cells (Hong et al., 2009).

iNKT cells are a unique subset of T cells that express a canonical invariant TCR α chain (Vα24-Jα18 in humans) and TCR β chains that use limited Vβ segments (Vβ11 in humans), and also play a key role in the regulation of innate and adaptive immunity (Berzins et al., 2011; Brennan et al., 2013). In contrast to conventional αβ T cells, iNKT cells recognize a limited number of lipid antigens presented by the MHC class I-like molecule CD1d. Stimulation of iNKT cells by α-galactosylceramide (α-GalCer), a synthetic glycosphingolipid, results in the rapid production of Th1 and Th2 cytokines (e.g., interleukin-γ [IFN-γ] and interleukin-4 [IL-4]) and increased expression of CD40 ligand (CD40L), which induces dendritic cell (DC) maturation

and production of IL-12p70 (Liu et al., 2008; McEwen-Smith et al., 2015; Uemura et al., 2009). These events ultimately lead to downstream activation of critical effectors of antitumor immunity, including NK cells, CTLs, and Th cells (Hong et al., 2009; Salio et al., 2014). Because CD1d is non-polymorphic, the modification of DC function by iNKT cells is independent of HLA restriction, making this process attractive for broad clinical application.

The antitumor potential of iNKT cells has been demonstrated in several clinical trials (Chang et al., 2005; McEwen-Smith et al., 2015; Motohashi et al., 2006, 2009; Nicol et al., 2011; Richter et al., 2013; Song et al., 2009; Uchida et al., 2008; Yamasaki et al., 2011). Infiltration of iNKT cells into tumor tissue is a favorable prognostic factor and is associated with improved survival, while low levels of circulating iNKT cells predict a poor clinical outcome (Molling et al., 2007). Although human iNKT cells are present wherever conventional T cells are found, their frequency relative to other T cells is less than 0.1%. In addition, a deficiency of iNKT cells and/or defects in their function has been reported in patients with many types of cancer (Berzins et al., 2011; Molling et al., 2005). Consequently, acquiring sufficient numbers of iNKT cells from patients to induce effective antitumor immune responses is currently an obstacle to iNKT cell-based immunotherapy.

A previous study has shown that iNKT cell TCR-harboring mouse iPSCs can differentiate into mature iNKT cells in vivo (Watarai et al., 2010). It remains unclear, however, whether human iNKT cell-derived iPSCs can differentiate into functional iNKT cells ex vivo. Here, we demonstrate that reprogramming human iNKT cells to pluripotency and subsequent re-differentiation of functional iNKT-like cells are possible ex vivo. These regenerated iNKT-like cells are functionally recovered and available in an unlimited supply from iPSCs. Moreover, they show both the expected adjuvant function of inducing leukemic antigen-specific polyclonal cytotoxic T cells via DC activation as well as TCR-independent direct killing of leukemic cell lines. This second feature is controlled by NKG2D signaling and, unexpectedly, DNAM-1 signaling, which is conceivably enhanced by the lack of TIGIT expression in the re-differentiated iNKT-like cells (re-iNKT cells). The adjuvant property and newly identified cytotoxic features of re-iNKT cells, which we demonstrate here against cancer cell lines, may have wide application in the field of immunotherapy.

RESULTS

iNKT Cell-Derived Human iPSCs Are Preferentially Generated from a CD4$^+$ Subset

Human iNKT cells can be classified into three phenotypically distinct subsets: CD4-positive (CD4$^+$), CD8-positive (CD8$^+$: CD8αβ or CD8αα), and CD4/8 double-negative (DN) (Brennan et al., 2013). The CD4$^+$ subset has the potential to produce a large amount of Th2 cytokines, while the DN and CD8$^+$ subsets have a Th1-biased profile. In addition, the CD8$^+$ subset produces more IFN-γ and more cytotoxicity than the CD4$^+$ or DN subsets. In this study, functionally distinct CD4$^+$ and DN iNKT cell lines were established from the peripheral blood of healthy donors and reprogrammed into iPSCs. We could not reprogram CD8$^+$ iNKT cells because of an insufficient number of cells obtained from donor peripheral blood. However, both CD4$^+$ and DN iNKT cells were efficiently transduced with defective Sendai virus vectors harboring four reprogramming factors, *OCT3/4*, *KLF4*, *SOX2*, and *C-MYC* (SeVdp(KOSM302L)) (Nishimura et al., 2011) and SV40 T antigen (SeV18 + SV40T/TS15ΔF) (Nishimura et al., 2013), and then formed into embryonic stem cell (ESC)-like colonies. However, most of the DN iNKT cell-derived colonies could not be maintained under the culture conditions used for human pluripotent stem cells, and those that were maintained showed no differentiation potential toward hematopoietic cells (Figures S1A and S1B). In addition, the rarely established ESC-like colonies derived from DN iNKT cells were positive for residual Sendai virus vector. In contrast, all established clones from CD4$^+$ iNKT cells were negative for residual transgenes (Figure S1C), showed pluripotency characterized by the expression of pluripotency-related genes (Figure S1D) and teratoma formation in immunodeficient mice (Figure S1E), and were confirmed to have a normal karyotype (Figure S1F). Although from different donors, all established clones showed the same TCRα chain with an invariant Vα24-Jα18 (*TRAV10*01-TRAJ18*01*) junctional sequence, which is a distinctive feature of human iNKT cells (Table 1).

Vα24-Jα18/Vβ11 TCR-Expressing T Cells Can Be Re-differentiated in the Presence of IL-15 and Expanded by TCR Stimulation

In contrast to conventional αβT cells, whose differentiation is controlled via TCR ligation by specific peptide antigens presented by polymorphic HLA molecules on thymic epithelial cells (Shah and Zuniga-Pflucker, 2014), iNKT cells differentiate in a unique fashion within the thymus (Godfrey et al., 2010). Once early T cell progenitors obtain the Vα24 invariant TCR at the CD4$^+$CD8$^+$ double-positive (DP) stage, they become sensitive to stimulation by specific glycolipid antigens presented by the non-polymorphic molecule CD1d. In addition, they become sensitive to self-stimulation by CD150, also known as SLAM (signaling lymphocytic activation molecule) (Veillette et al., 2007). Cytokine dependency during differentiation differs slightly between αβT

Table 1. Junction Sequences of TCR Genes in Reprogrammed and Redifferentiated Cells

Clone	Productivity	TRAV	TRAJ	3′ Va	P(N)	5′ Ja	Frequency
V-J Junction Sequence of Rearranged TRA Genes in the Genome of CD4$^+$ iNKT-iPSC							
1	productive	10*1	18*01	TGTGTGGTGAGCG		ACAGAGGCTCAACCCTGGGGAGGCTATACTTT	5/8 productive
	productive	30*01	10*01	TG	TGGCACAGAGAGG	ACGGGAGGAGGAAACAAACTCACCTTT	3/8 productive
2	productive	10*01	18*01	TGTGTGGTGAGC		GACAGAGGCTCAACCCTGGGGAGGCTATACTTT	1/1 productive
4	productive	10*01	18*01	TGTGTGGTGAGC		GACAGAGGCTCAACCCTGGGGAGGCTATACTTT	1/1 productive
8	productive	10*01	18*01	TGTGTGGTGAGCG		ACAGAGGCTCAACCCTGGGGAGGCTATACTTT	5/10 productive
	productive	30*01	10*01	TG	TGGCACAGAGAGG	ACGGGAGGAGGAAACAAACTCACCTTT	5/10 productive
V-J Junction Sequence of Rearranged TRA mRNAs of Re-iNKT Cells							
1	productive	10*1	18*01	TGTGTGGTGAGCG		ACAGAGGCTCAACCCTGGGGAGGCTATACTTT	9/13 productive
	productive	30*01	10*01	TG	TGGCACAGAGAGG	ACGGGAGGAGGAAACAAACTCACCTTT	4/13 productive
2	productive	10*01	18*01	TGTGTGGTGAGC		GACAGAGGCTCAACCCTGGGGAGGCTATACTTT	5/5 productive
4	productive	10*01	18*01	TGTGTGGTGAGC		GACAGAGGCTCAACCCTGGGGAGGCTATACTTT	2/2 productive
8	productive	10*01	18*01	TGTGTGGTGAGCG		ACAGAGGCTCAACCCTGGGGAGGCTATACTTT	6/12 productive
	productive	30*01	10*01	TG	TGGCACAGAGAGG	ACGGGAGGAGGAAACAAACTCACCTTT	6/12 productive

Clone	Productivity	TRBV	TRBD	TRBJ	3′ Vb	N1-P-Db-N2	5′ Jb	Frequency
V-D-J Junction Sequence of Rearranged TRB Genes in Genome of CD4$^+$ iNKT-iPSC								
1	productive	25-1*01	1*01	1-5*01	TGTGCCAGCAGTGAA	CTAGGGGAGAATTTG	CAGCCCCAGCATTTT	6/6 productive
	unproductive	–	1*01	1-6*01	–	GGGTGCCGATGGAAT	TTCACCCCTCCACTTT	
2	productive	25-1*01	1*01	2-3*01	TGTGCCAGCAGTG	GCAGGAGCCTAAA	CACAGATACGCAGTATTTT	2/2 productive
	unproductive	germline	1*01	2-7*01	TACAAAGCTGTAACATTGTG	GGGACAGGGGGCCGC	TCCTACGAGCAGTACTTCGGGCCGG	
4	productive	25-1*01	1*01	2-3*01	TGTGCCAGCAG	GGGATCCGGGACAGGGGCC	GATACGCAGTATTTT	4/4 productive
	unproductive	11-1*01	–	2-6*01	GGCAG	–	CAGG	
8	productive	25-1*01	1*01	1-5*01	TGTGCCAGCAGTGAA	CTAGGGGAGAATTTG	CAGCCCCAGCATTTT	6/6 productive
	unproductive	–	1*01	1-6*01	–	GGGTGCCGATGGAAT	TTCACCCCTCCACTTT	
V-D-J Junction Sequence of Rearranged TRB mRNAs of Re-iNKT Cells								
1	productive	25-1*01	1*01	1-5*01	TGTGCCAGCAGTGAA	CTAGGGGAGAATTTG	CAGCCCCAGCATTTT	5/5 productive
2	productive	25-1*01	1*01	2-3*01	TGTGCCAGCAGTG	GCAGGAGCCTAAA	CACAGATACGCAGTATTTT	5/6 productive
	productive	12-3*01	2*01	2-3*01	TGTGCCAGCAGTT	CTTCATCCACTCCCGTC	GATACGCAGTATTTT	1/6 productive
4	productive	25-1*01	1*01	2-3*01	TGTGCCAGCAG	CGGATCCGGGACAGGGGCC	GATACGCAGTATTTT	5/5 productive
	unproductive	7-9*04	1*01	2-1*01	AGAGA	CACAGGCAGGGAA	GGGCC	
	unproductive	20-1*03	–	2-2P*01	GATGG	–	AGAGG	
8	productive	25-1*01	1*01	1-5*01	TGTGCCAGCAGTGAA	CTAGGGGAGAATTTG	CAGCCCCAGCATTTT	6/7 productive
	productive	20-1*01	2*01	2-7*01	TGCAGTGCTAGA	TCCTACTTGGGGGGAGAA	GAGCAGTACTTC	1/7 productive

and iNKT cells, as IL-15 is crucial for iNKT cell differentiation (Gordy et al., 2011). When iNKT-iPSCs were differentiated into T-lineage cells without IL-15, they stayed at the CD4$^-$CD8$^-$ DN stage but were partially positive for iNKT cell-related molecules, including CD56, CD69, CD161 (NKRP1; NK cell-related protein 1), CD314 (cellular

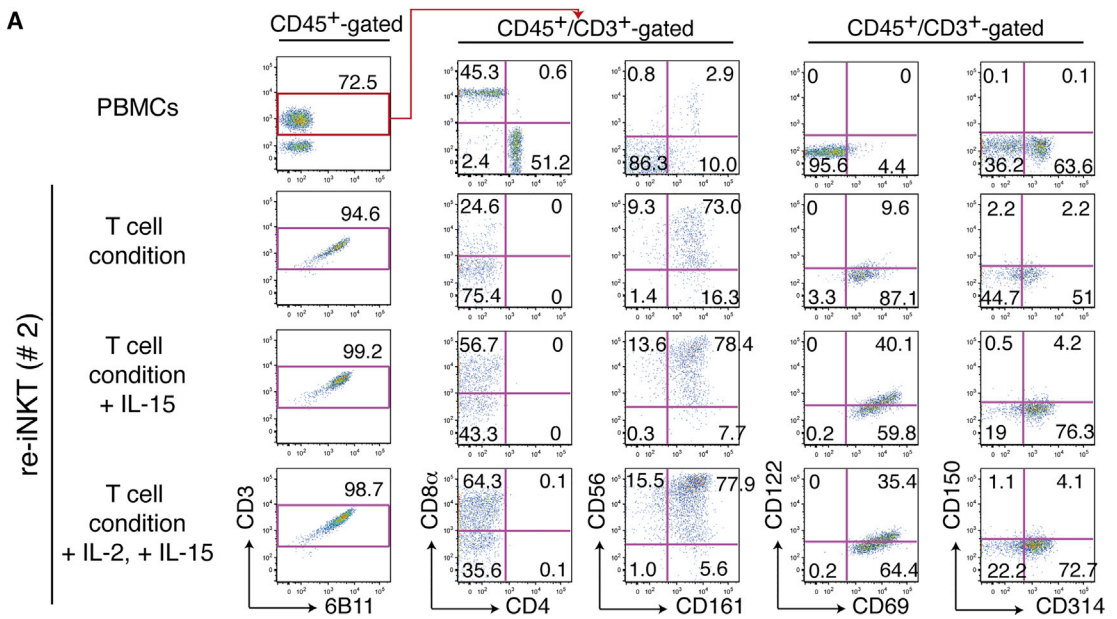

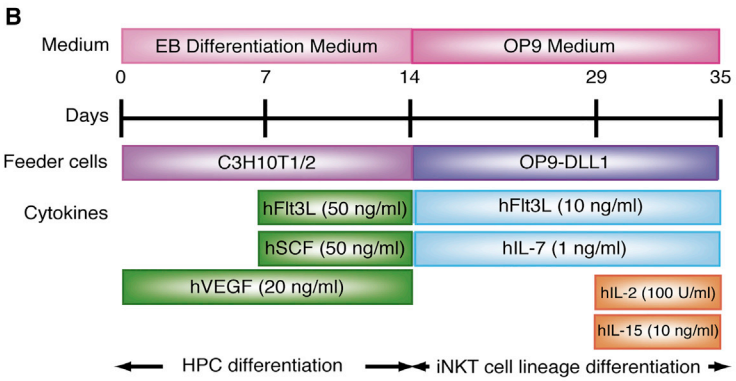

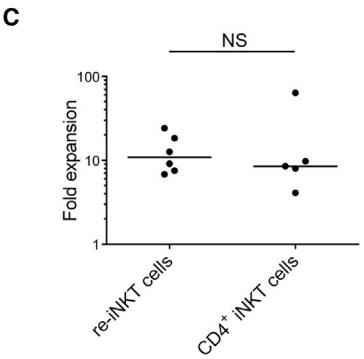

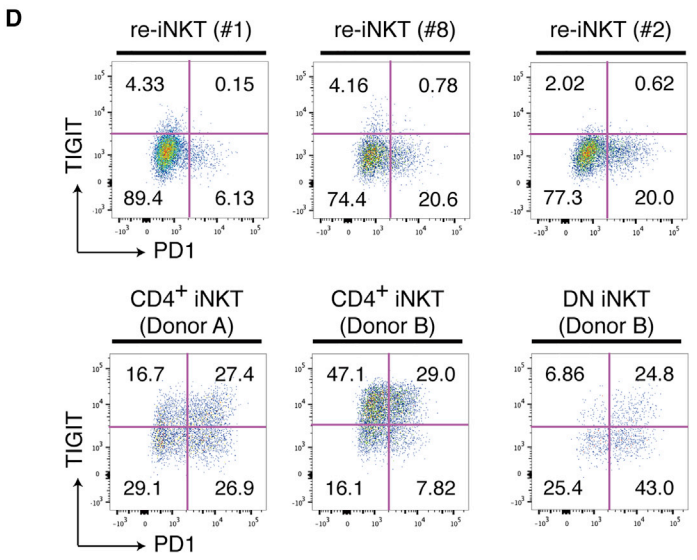

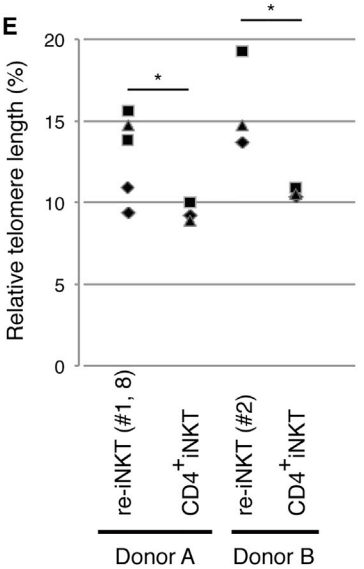

(legend on next page)

stress-ligand receptor NKG2D), and invariant TCR (stained by 6B11, a monoclonal antibody (mAb) specific for the invariant Vα24-Jα18 CDR3 loop), and expressed low levels of CD150 and CD122 (IL-2/-15 receptor β chain) at the third week of culture on OP9/DL1 (Figure 1A). Although they expressed invariant TCR, iPSC-derived differentiating cells showed minimal expansion upon stimulation by α-GalCer-loaded peripheral blood mononuclear cells (PBMCs) (data not shown). This prompted us to speculate whether other signals, such as IL-15 and/or SLAM-SLAM interaction, were necessary for further maturation. In light of the positive feedback effect of IL-15 signaling on CD122 expression (Castillo et al., 2010), which may induce further maturation, we modified the culture medium, adding 10 ng/ml IL-15 from the second or third week of culture on OP9/DL1. Improving the culture conditions led to greater numbers of invariant TCR-positive cells, and a fraction of these cells showed further enhancement of CD56, CD69, CD122, CD150, CD161, and CD314 expression (Figure 1A). It is generally difficult to exactly identify control/check points (the expressions of TCR or NK markers) or immature stages in the differentiation process (Godfrey and Berzins, 2007), since the differentiation of TCR pre-rearranged iPSC-derived hematopoietic cells into T-lineage cells on OP9/DL1 deviates from normal T-lymphopoiesis (Nishimura et al., 2013; Vizcardo et al., 2013). We were able to confirm, however, that additional IL-15 induced further maturation past control/check point 2 to differentiating cells (Figures S2A and S2B). By adding IL-2 to the culture, we increased cell numbers 7.5-fold over that seen with IL-15 alone ($n \geq 3$). In subsequent experiments, therefore, we cultured re-differentiated T cells with a combination of Flt3L (FMS-like tyrosine kinase 3 ligand), IL-7, IL-2, and IL-15 (Figure 1B).

Vα24-Jα18/Vβ11 TCR-expressing re-differentiated T cells were stained with α-GalCer/CD1d tetramer to the same degree as the parental iNKT cells (Figure S2C) and were responsive to stimulation with α-GalCer-pulsed PBMCs. Although there were some differences in the responsiveness to stimulation among iNKT-iPSC clones, the final yield after around 2 weeks was nearly the same as that of the parental iNKT cells (Figure 1C). In addition, repeated stimulation with α-GalCer-pulsed PBMCs or the mitogen phytohemagglutinin (PHA-P) in vitro resulted in expansion of the initial cell number by about 10^3- to 10^4-fold (Figure S2D). Because of their phenotypic and functional similarity to iNKT cells, the re-differentiated T cells expressing Vα24-Jα18/Vβ11 TCR are hereafter referred to as "re-iNKT cells."

Generation of iNKT-like Cells through Reprogramming

Based on previous reports (Johnston et al., 2014; Postow et al., 2015) and our previous observations of $CD8^+$ T cell rejuvenation through reprogramming (Nishimura et al., 2013), we estimated reprogramming-mediated functional recovery by comparing the expression of the immunological exhaustion-related checkpoint proteins PD-1 (programmed cell death protein 1) and TIGIT (T cell immunoreceptor with immunoglobulin and ITIM domains) and cell exhaustion-related telomere length in expanded re-iNKT cells with those in parental $CD4^+$ and DN iNKT cells. Middle to high expression of PD-1 and TIGIT was observed in both $CD4^+$ and DN iNKT cells, whereas re-iNKT cells expressed minimal levels of PD-1 and almost no TIGIT, even after several cycles of expansion induced by TCR stimulation (Figure 1D). The re-iNKT cells also showed a recovery of telomere length as previously reported (Nishimura et al., 2013) (Figure 1E).

Figure 1. Re-differentiation of iNKT Cells from iNKT-iPSCs

(A) Surface antigen profiles of re-differentiating T cells from $CD4^+$ iNKT-iPSC (clone 2) on OP9/DL1 feeder cells on day 21 in the presence of the indicated cytokines. The results shown are representative of four independent experiments examining the surface protein expression patterns of the cells gated by CD45, CD3, and 6B11.

(B) Schematic illustration showing the culture protocol for iNKT cell re-differentiation from $CD4^+$ iNKT cell-derived iPSCs. EB differentiation medium: Iscove's modified Dulbecco's medium supplemented with 15% fetal bovine serum and a cocktail of 10 μg/ml human insulin, 5.5 μg/ml human transferrin, 5 ng/ml sodium selenite, 2 mM L-glutamine, 0.45 mM monothioglycerol, and 50 μg/ml ascorbic acid. OP9 medium: α-MEM supplemented with 15% FBS, 2 mM L-glutamine, 100 U/ml penicillin, and 100 μg/ml streptomycin.

(C) Fold expansion of parental $CD4^+$ iNKT cells and newly induced re-iNKT cells around 2 weeks after stimulation with α-GalCer-pulsed PBMCs. The result obtained with each indicated cell in three independent experiments is shown as a filled circle. Experiment 1: clone 2, parental clone and subclone of donor A; experiment 2: clone 1, clone 8, and donor A; experiment 3: clone 1, clone 2, clone 8, and parental clones of donor A and B. Horizontal lines indicate medians. NS, not significant.

(D) Co-expression profile of PD-1 and TIGIT on re-iNKT cells and parental iNKT cells after TCR stimulation (gated by CD45, CD3, and 6B11). The results shown are representative of two independent experiments. The numbers in the quadrants indicate percentages of cells.

(E) Telomere length in parental $CD4^+$ iNKT cells and induced re-iNKT cells normalized to the tetraploid leukemic cell line 1301. Datasets from three independent experiments that include data from three different re-iNKT cell clones (1, 2, and 8), and two parental iNKT cell clones (donor A and donor B) are shown as filled diamonds, squares, and triangles, respectively. t Tests for paired data were used to compare results from the same donor; $^*p < 0.05$.

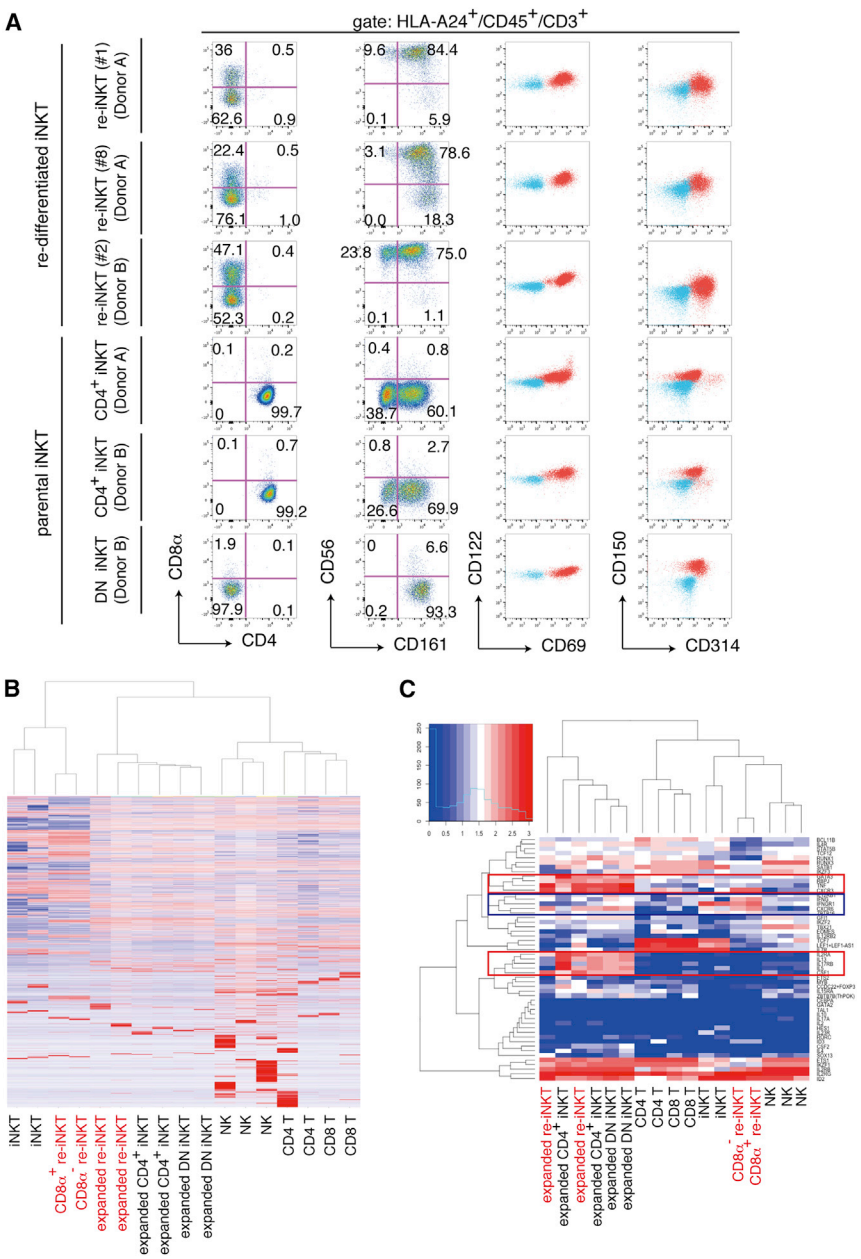

Figure 2. Gene and Molecular Expression Profile of Re-iNKT Cells

(A) Flow cytometric analysis of T cells re-differentiating from CD4$^+$ iNKT-iPSCs on day 10 after TCR stimulation. iPSC-derived re-differentiating cells were stimulated with α-GalCer-pulsed (10 ng/ml) and irradiated PBMCs from an HLA-A24-negative donor. The results shown are the surface protein expression patterns of re-differentiating cells gated by HLA-A24, CD45, CD3, and 6B11, and are representative of four experiments. The blue and red populations in the right two panels respectively indicate unstained and stained samples for the indicated molecules.

(B and C) Global gene expression profiles (B) and two-way clustering of 53 selected gene expression profiles (C) related to NK/T cell differentiation and function for re-iNKT cells (clones 2 and 4; both from donor B) and primary immune cells. Levels of mRNA expression in re-iNKT cells and primary immune cells were determined using RNA sequencing. Heatmaps show the differential expression of genes among samples. Red and blue indicate increased and decreased expressions, respectively. Blue and red boxes in (C) indicate gene clusters preferentially up-regulated in resting and activated re-iNKT cells, respectively.

Gene and Protein Expression Profiles Predict Re-iNKT Cells to Have the Potential of CD4$^+$ iNKT Cells but Are Biased toward the Th1-like Phenotype

All expanded re-iNKT cells showed invariant TCR expression (Figure S2B and Table 1) and expressed CD122 and CD150 at similar levels. In addition, the activation- and cytotoxicity-associated molecules CD56, CD69, CD161, and CD314 were detected in most of the expanded re-iNKT cells (Figure 2A). Re-iNKT cells also changed their expression dominance from CD45RA to CD45RO during α-GalCer-based stimulation, consistent with the effector memory phenotype (Figure S2E). Although re-iNKT cells were originally generated from CD4$^+$ iNKT cells, their surface phenotype was more similar to DN iNKT cells. We therefore analyzed the global gene expression profiles of re-iNKT cells and other primary lymphoid cell subsets. Hierarchical clustering of transcriptomes enabled by mRNA sequencing indicated that re-iNKT cells are closest to freshly isolated iNKT cells and next closest to expanded iNKT cells after TCR stimulation (Figure 2B). This relationship was confirmed by the hierarchical clustering of selected genes related to NK/T cells, including 30 transcription factors, 13 cytokines, and ten cytokine receptors (Figures 2C and Table S1). Several genes known to characterize

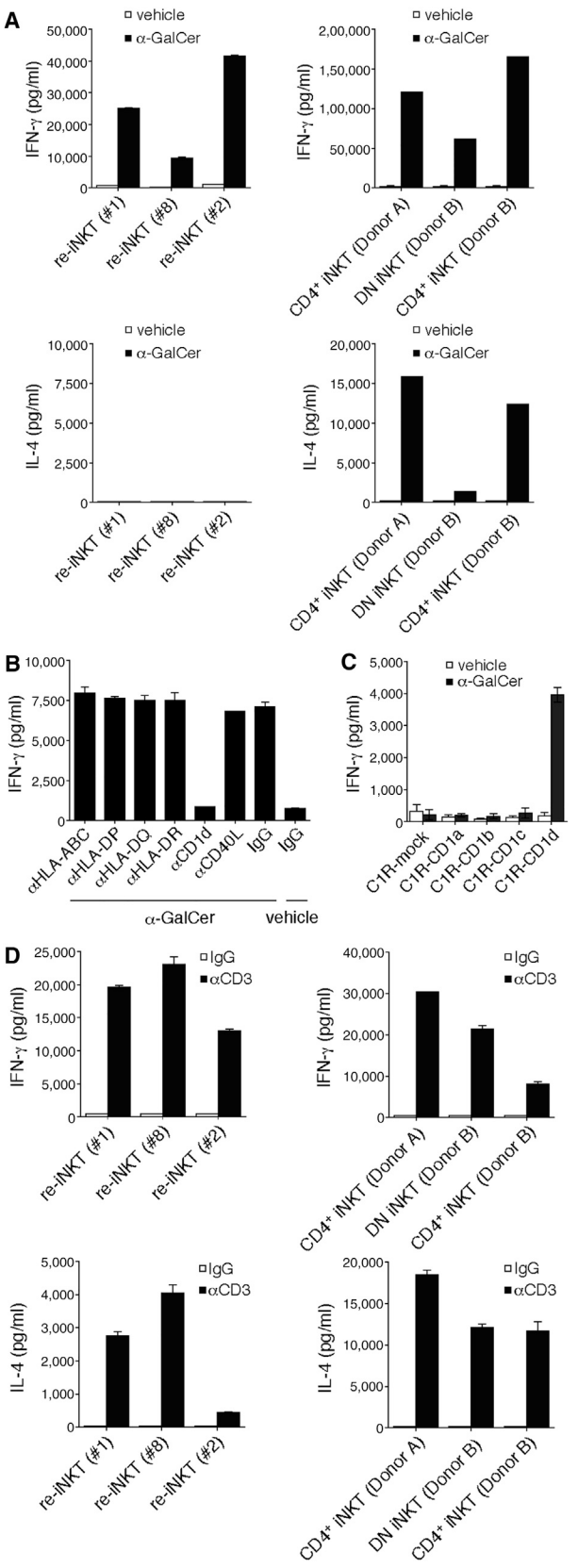

Figure 3. CD1d-Restricted, α-GalCer-Specific Response and Cytokine Profile of Re-iNKT Cells

(A) IFN-γ and IL-4 production. Re-iNKT cells or parental iNKT cells were co-cultured with DCs in the presence of vehicle or 100 ng/ml α-GalCer.

(B) Re-iNKT cells were cultured with α-GalCer DCs in the presence of the indicated blocking Abs. Blockade was assessed based on IFN-γ production.

(C) α-GalCer-dependency and CD1d-restriction. Re-iNKT cells were cultured with C1R cells expressing mock or the indicated molecules in the presence of vehicle or 100 ng/ml α-GalCer.

(D) Cytokine profiles. Re-iNKT cells or parental iNKT cells were stimulated for 24 hr with plate-bound control immunoglobulin G (IgG) or anti-CD3 mAb (10 μg/ml), after which levels of the indicated cytokines in the culture supernatants were evaluated.

Data were run in triplicate, and the experiment was repeated three times. The results of one representative experiment are shown. Error bars depict mean ± SD.

iNKT cells, including the innate lymphoid cell-related transcription factor *ZBTB16* and the Th1 type pro-inflammatory cytokine and receptor genes *IFNG*, *IFNGR1*, and *IL-12RB1*, were preferentially expressed in re-iNKT cells before TCR stimulation (Figure 2C, blue box). On the other hand, the Th2 helper T cell-related transcription factor *GATA3*, the Notch signal-related transcription factor *RBPJ*, and the NK/T cell-related cytokine and receptor genes *TNF*, *IL-5*, *IL-13*, *CSF1*, and *IL2RA* were preferentially expressed in activated re-iNKT cells and expanded primary iNKT cells (Figure 2C, red boxes). Taken together, these findings indicate that although re-iNKT cells show a DN iNKT cell-like surface phenotype, their expression profile covers $CD4^+$ iNKT cell-related Th1 and Th2 type genes.

Microarray-based DNA methylation analysis was performed to evaluate the epigenetic status of re-iNKT cells. Correlation plots indicated that the methylation level of re-iNKT cells was generally higher than that of original $CD4^+$ or DN iNKT cells, which were similar (Figure S3A). A detailed profile of each gene revealed that master transcriptional factors of iNKT cells, such as *ZBTB16*, *TBX21*, and *GATA3*, were similarly methylated among the three cell populations. Th1-related cytokine genes such as tumor necrosis factor α (TNF-α) and IFN-γ were also similarly methylated among the populations, but Th2-related cytokine genes such as *IL-4* and *IL-5* were preferentially methylated in re-iNKT cells. The hypermethylation of *CD4* gene could contribute to the absence of CD4 expression in $CD4^+$ iNKT-iPSC-derived re-iNKT cells (Figure S3B).

When DCs were used as antigen-presenting cells (APCs), re-iNKT cells produced IFN-γ and negligible amounts of IL-4 (Figure 3A), and the IFN-γ production was inhibited by the addition of a blocking mAbs specific for CD1d (Figure 3B). CD1d restriction was also confirmed by using

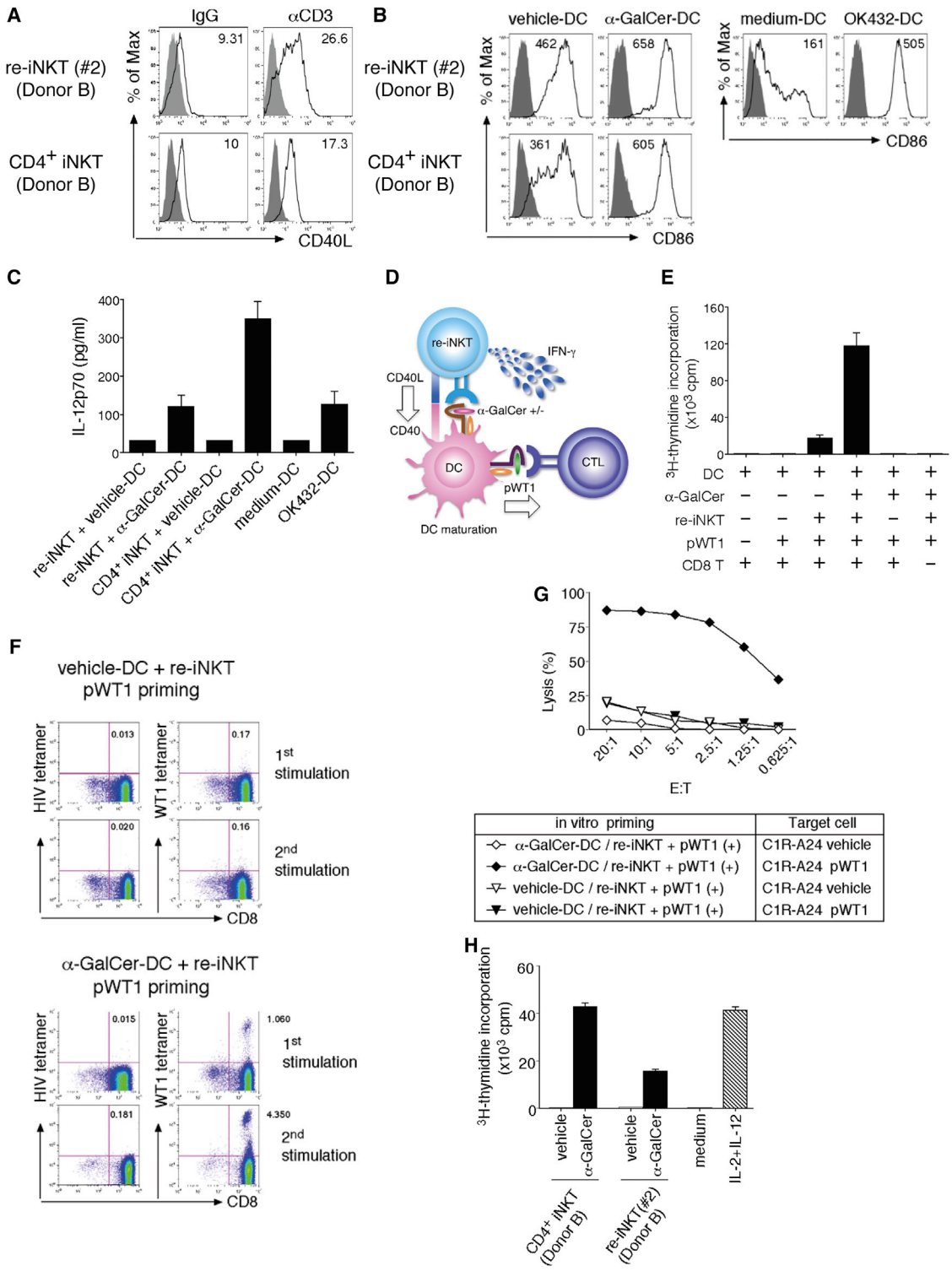

Figure 4. Induction of Tumor Antigen-Specific CTLs via Re-iNKT Cell-DC Interaction

(A) Re-iNKT cells or parental iNKT cells were stimulated with plate-bound anti-CD3 mAb, after which CD40L expression was evaluated. The mean fluorescence intensity (MFI) of CD40L is shown.

(B) Vehicle- or α-GalCer DCs were cultured with re-iNKT cells at a DC/re-iNKT cell ratio of 10:1, after which CD86 expression on DCs was evaluated. The MFI of CD86 is shown. Medium DCs and OK432 DCs served as references.

(legend continued on next page)

C1R-CD1d as the APC (Figure 3C). When anti-CD3 mAb was used for TCR stimulation, re-iNKT cells produced both Th1 and Th2 cytokines, including IL-2, IL-4, IL-5, IL-13, GM-CSF (granulocyte macrophage colony-stimulating factor), IFN-γ, and TNF-α, just as parental $CD4^+$ iNKT cells do (Figures 3D and S4). The IFN-γ/IL-4 ratio in re-iNKT cells stimulated with anti-CD3 mAb was higher than that in parental iNKT cells, indicating that re-iNKT cells had a more Th1-biased profile than the parental cells (Figures 3A, 3D, and S4).

Activation of Re-iNKT Cells Induces DC Maturation and Downstream Activation of Both Cancer Antigen-Specific CTLs and NK Cells

iNKT cells significantly influence the efficacy of immune responses by modulating DC function. CD40L molecules expressed by activated iNKT cells stimulate DCs through CD40 ligation, which induces DC maturation characterized by CD80 (B7-1) and CD86 (B7-2) elevation following IL-12p70 production (Brennan et al., 2013). IL-12p70 is a strong NK cell activator and a crucial inducer of functional antigen-specific Th1 cells and CTL responses (Trinchieri, 2003). We initially confirmed that the stimulation of TCRs on re-iNKT cells using immobilized anti-CD3 mAb activated the cells and enhanced surface CD40L expression (Figure 4A). Thereafter, vehicle DCs or α-GalCer DCs were co-cultured with re-iNKT cells, and the expression of the co-stimulatory molecule CD86 along with IL-12p70 production in the differentially conditioned DCs was evaluated (Figures 4B and 4C). α-GalCer DCs conditioned by re-iNKT cells (re-iNKT/α-GalCer DCs) expressed higher levels of CD86 than re-iNKT/vehicle DCs, and re-iNKT/α-GalCer DCs produced IL-12p70, although at a level lower than that produced by α-GalCer DCs conditioned by the parental iNKT cells (iNKT/α-GalCer DCs) (Figure 4C). In addition, the IL-12p70 production could be inhibited using a blocking anti-CD1d or anti-CD40L mAb (Figure S5A). These findings indicate that activated re-iNKT cells are able to induce DC maturation and IL-12p70 production via CD40 ligation.

Studies have shown that iNKT cells act via DCs to provide help in priming diverse, tumor antigen-specific $CD8^+$ T cells (Brennan et al., 2013). Functional re-iNKT cells would be extremely useful for preventing tumor escape from antigen-specific monoclonal CTLs through tumor antigen mutagenesis if functionality could be confirmed. We therefore performed CTL priming experiments using a representative cancer antigen, Wilms' tumor 1 (WT1) (Figure 4D) (Cheever et al., 2009). Initially, re-iNKT cells were co-cultured with vehicle DCs or α-GalCer DCs to induce DC maturation. The DCs were then loaded with an HLA-A*24:02-restricted, modified 9-mer peptide derived from WT1 ($WT1_{235–243}$), irradiated, and cultured with autologous $CD8^+$ T cells for antigen-specific priming of CTLs. After 6 days of culture, we observed markedly greater proliferation of $WT1_{235–243}$-tetramer-positive $CD8^+$ T cells in cultures stimulated by $WT1_{235–243}$ peptide-loaded α-GalCer DCs than in cultures stimulated by $WT1_{235–243}$ peptide-loaded vehicle DCs (Figures 4E, 4F, and S5B). Moreover, the CTLs induced by $WT1_{235–243}$ peptide-loaded α-GalCer DCs exhibited cytotoxic activity toward $WT1_{235–243}$ peptide-loaded HLA-$A24^+$ C1R cells, but not toward vehicle-loaded HLA-$A24^+$ C1R cells (Figure 4G). These data indicate that re-iNKT cells activated by α-GalCer exert cellular adjuvant effects that boost tumor antigen-specific polyclonal CTL responses via DCs and could be useful for developing re-iNKT cell-based adjuvant therapies. Another important function of iNKT cells is that they have the potential to induce downstream activation of NK cells via interaction with α-GalCer-loaded DCs. As indicated in Figures 4H and S5C, NK cells up-regulated the activation marker CD69 and showed effective expansion in the presence of supernatant from re-iNKT cell/α-GalCer-loaded DC interaction.

Re-iNKT Cells Show NK Cell-like Cytotoxic Activity through a Mechanism Dependent on NKG2D and Enhanced DNAM-1 Pathways

Earlier studies indicate that iNKT cells exhibit perforin- or TRAIL-mediated cytotoxicity toward some hematopoietic

(C) IL-12p70 production by DCs stimulated using the indicated conditions.
(D) Schematic representation of the $WT1_{235–243}$-specific CTL priming assay.
(E and F) Vehicle- or α-GalCer DCs were cultured with or without re-iNKT cells (clone 2). Differentially conditioned DCs were irradiated and cultured with autologous $CD8^+$ T cells ± $WT1_{235–243}$ peptide. (E) Proliferative responses were measured as $[^3H]$thymidine incorporation.
(F) Increased frequencies of $WT1_{235–243}$-specific CTLs after repeated stimulation were determined using WT1 tetramer. HIV tetramer served as a negative control.
(G) Cytotoxic activities of pWT1-primed $CD8^+$ T cells toward C1R-A*24:02 cells ± WT1 peptide were determined using ^{51}Cr-release assays at the indicated E/T ratios.
(H) Proliferative responses of NK cells (1.0×10^5) cultured for 48 hr in the presence of 25% cell-free supernatants that were from iNKT-DC co-culture. Medium control and IL-2 (300 IU/ml) plus IL-12 (20 ng/ml) control served as references.
In (A), (B), (F), and (G), one representative result from at least two independent experiments is shown. In (C), (E), and (H) data were run in triplicate, and experiments were repeated at least twice; the results of one representative experiment are shown. Error bars depict mean ± SD.

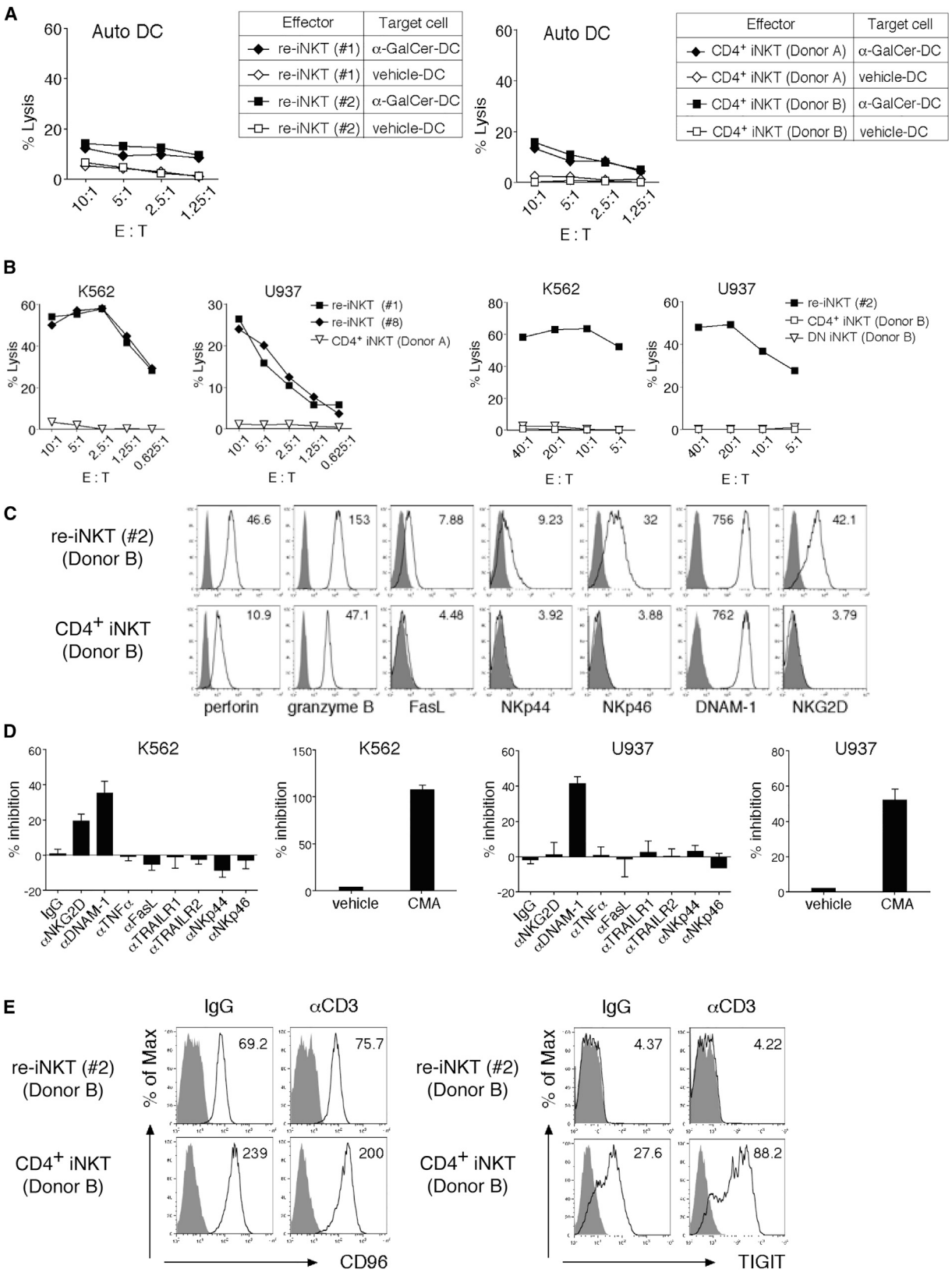

(legend on next page)

malignancies and DCs (Metelitsa et al., 2003; Nicol et al., 2000; Nieda et al., 2001; Takahashi et al., 2000). In addition, certain NKG2D-expressing DN iNKT cell subsets kill K562 NK-sensitive cells, which lack CD1d and HLA-I but are rich in the NKG2D ligands MICA and MICB, and also express ULBP2 and ULBP4 (Kuylenstierna et al., 2011). Because the major re-iNKT cell population expresses NKG2D as well as CD56 and CD161, two other NK markers, we evaluated the cytotoxic potential of re-iNKT cells in vitro using ^{51}Cr-release assays. Like the parental iNKT cells, re-iNKT cells displayed minimal cytotoxic activity toward vehicle-pulsed DCs (vehicle DCs) and only weak cytotoxicity toward α-GalCer-pulsed DCs (α-GalCer DCs) (Figure 5A). However, in contrast to the parental iNKT cells, which exhibited little cytotoxicity toward K562 or U937 cells, re-iNKT cells showed remarkable cytotoxic activity, even at low effector/target (E/T) ratios (Figure 5B). On the other hand, re-iNKT cells showed only weak cytotoxicity toward Daudi cells, which lack NKG2D ligands such as MICA/B, ULBP1, ULBP2, and ULBP3, and DNAM-1 ligands such as poliovirus receptor (PVR; CD155) or nectin-2 (PVRL; CD112) (Figures S6A and S6B). Both re-iNKT cells and parental iNKT cells expressed intracellular perforin and granzyme B as well as surface DNAM-1 (CD226) (Figure 5C). However, the expression of Fas ligand (FasL; CD178), natural cytotoxicity receptors (NCRs; NKp44 and NKp46), and NKG2D was restricted to re-iNKT cells and was absent from parental CD4$^+$ NKT cells (Figure 5C). Blocking experiments revealed that re-iNKT cells mediated perforin-, NKG2D-, and DNAM-1-dependent K562 cell lysis, while U937 cell lysis induced by re-iNKT cells was mediated mainly by perforin and DNAM-1 (Figure 5D). These data suggest that re-iNKT cells can kill cancer cells via NKG2D- and DNAM-1-dependent mechanisms.

Because DNAM-1 is expressed in both re-iNKT cells and parental iNKT cells (Figure 5C), we asked why DNAM-1-mediated cytotoxicity was restricted to re-iNKT cells. The ligands for DNAM-1, PVR, and nectin-2 share with CD96 and TIGIT an inhibitory receptor important for the modulation of NK cell or CTL function. Both CD96 and TIGIT attenuate effector responses by competitively inhibiting or interfering with DNAM-1-mediated co-stimulation of CTLs (Chan et al., 2014; Johnston et al., 2014). Flow cytometric analysis revealed that TIGIT is strongly expressed on parental iNKT cells but never on re-iNKT cells, whereas CD96 is expressed on both (Figures 1D and 5E). These findings suggest that weak expression of TIGIT on re-iNKT cells may be crucial for enhanced DNAM-1-mediated target cell killing and that re-iNKT cells exert cytotoxicity through this mechanism, which is unlike parental iNKT cells.

DISCUSSION

In this study, we demonstrated the regeneration and expansion of human iNKT cells via iPSCs. Re-iNKT cells were originally induced from CD4$^+$ iNKT cells, although re-iNKT cells were CD4$^-$CD8$^-$ DN and exhibited Th1-biased properties and cytotoxicity. One possible explanation for this phenotype is that it reflects the effect of IL-15, which is reportedly indispensable for the proper development and terminal maturation of iNKT cells (Gordy et al., 2011). Indeed, our established protocol, in which exogenous IL-15 was added, achieved differentiation and functional maturation of re-iNKT cells through the up-regulation of T-bet, which accelerates IL-2/-15Rβ expression, leading to differentiation of Th1-biased re-iNKT cells via a positive feedback effect of IL-15 signaling. The re-differentiation may depend in part on the aberrant differentiation of progenitor T cells into mature re-iNKT cells. Specifically, iNKT cells derived from iPSCs never exhibit a CD4$^+$CD8$^+$ DP stage during in vitro differentiation, which suggests re-iNKT cells skip that physiological step of iNKT

Figure 5. NKG2D- and DNAM-1 Mediated TCR-Independent Cytotoxicity of re-iNKT Cells

Parental CD4$^+$ iNKT cells and re-iNKT cells were stimulated with irradiated PBMCs pulsed with α-GalCer in the presence of rhIL-2 and rhIL-15 and then expanded and used for the assays.

(A) Cytotoxicity of re-iNKT cells and parental CD4$^+$ iNKT cells toward autologous vehicle DCs and α-GalCer DCs at the indicated E/T ratios.

(B) Cytotoxicity of re-iNKT cells and parental CD4$^+$ iNKT cells toward K562 and U937 cells at the indicated E/T ratios.

(C) Expression of cytotoxicity-related molecules in IL-2-pretreated re-iNKT cells or parental iNKT cells. Expression of the indicated molecules (open) and isotype-matched controls (filled) is shown. The MFI of each molecule is shown in the upper right corner.

(D) Cytotoxicity toward the indicated tumor cell lines at an E/T ratio of 2.5:1 was tested in the presence of the indicated Abs blocking receptor/ligand interactions or after pretreating re-iNKT cells with 10 nM concanamycin A (CMA) to block perforin.

(E) CD96 and TIGIT expression. Re-iNKT cells or parental iNKT cells were stimulated with plate-bound control IgG or anti-CD3 mAb (10 μg/ml). Expression of the indicated molecules (open) and isotype-matched controls (filled) is shown. The MFI of each molecule is shown in the upper right corner.

In (C) and (E), one representative result from two to three independent experiments is shown. In (D), data were run in triplicate, and experiments were repeated twice; the results of one representative experiment are shown. Error bars depict mean ± SD.

cell differentiation. It is known that some lymphoid cells with innate-like immune functionality are directly derived at the $CD4^-CD8^-$ DN progenitor T cell stage under the control of the transcriptional repressor ID2. These innate lymphoid cells, which include NK cells, have been characterized by their effector functionality, and some exhibit $CD4^+$ T helper cell-like functions that are also observed in iNKT cell subsets (Brennan et al., 2013; Eberl et al., 2015). At the moment, we do not know whether the normal counterpart of re-iNKT cells is within the innate lymphoid subsets. Further investigation to clarify the mechanism of re-iNKT cell differentiation will improve the protocol to generate re-iNKT cells that are completely equivalent to natural iNKT cells.

It is often pointed out that tumor cells can escape immune cells by changing their antigenicity through the modification of targeted peptide sequences or reduction of HLA-molecule expression (Schreiber et al., 2011). This is usually the case when immune therapies with antigen-specific monoclonal CTLs fail. Given their functional similarity to natural iNKT cells, re-iNKT cells, which would be available at an unlimited supply, would be expected to exert cellular adjuvant effects via DCs following the activation of tumor antigen-specific polyclonal CTLs and NK cells, although the level of cytokine production induced by α-GalCer DCs was lower in re-iNKT than in parental cells and there was less cytokine variety. In addition, the NK cell-like cytotoxicity of re-iNKT cells could assist with TCR-independent antitumor responses via NKG2D- and DNAM-1-mediated direct killing of tumor cells. TIGIT inhibits DNAM-1 function via the same ligands not only by competitively inhibiting ligand binding but also through direct interaction with DNAM-1, which physically prevents DNAM-1 homodimerization (Johnston et al., 2014; Stanietsky et al., 2009; Yu et al., 2009). The balance between DNAM-1 and TIGIT expression may control iNKT cell cytotoxicity; that is, re-iNKT and parental iNKT cells express equal levels of DNAM-1, but re-iNKT cells do not express TIGIT, which may enable stronger cytotoxic signaling than primary iNKT cells. In addition, TIGIT was recently identified as a new exhaustion marker expressed in tumor-infiltrating lymphocytes and is thought to be an attractive candidate for blockade, along with PD-1, to reverse CTL dysfunction in cancer (Johnston et al., 2014). That re-iNKT cells scarcely express TIGIT and PD-1 is a property that would be beneficial for cells used in cancer immunotherapy. In addition, iNKT cells reportedly control the tumor microenvironment by killing tumor-associated macrophages (Song et al., 2009) and converting myeloid-derived suppressor cells into APCs (De Santo et al., 2010). The general mechanism of the direct killing activity in re-iNKT cells is unknown. The low expression and hypermethylation of *BCL11B* may be partly responsible (Figures 2C and S3B), as the loss of the *Bcl11b* expression induces lineage reprogramming from murine T cells to NK cells (Li et al., 2010). Thus, Th1-biased cytokine production and direct TCR-independent killing may enable re-iNKT cells to exert therapeutic effects against the tumor microenvironment. Nevertheless, it will be important to gather additional therapeutic evidence in vitro and in vivo using appropriate animal models, as the characteristics and responsiveness of the re-iNKT cells were not completely identical to those of parental iNKT cells.

iNKT cells have been implicated in the regulation of immune responses associated with a broad range of diseases, including autoimmunity, infectious diseases, and cancer, and their contribution to cell therapy has been much anticipated. Although many technical challenges lie ahead, re-iNKT cells are expected to open new avenues toward broadly applicable iNKT cell-based immunotherapies.

EXPERIMENTAL PROCEDURES

Preparation of Vα24 iNKT Cells and Generation of iNKT-iPSCs

The preparation of human iNKT cells was as described previously (Liu et al., 2008). In brief, PBMCs from three healthy donors were cultured for 15 days in the presence of 10 ng/ml α-GalCer, after which $V\alpha24^+6B11^+CD4^-CD8\beta^-$ or $V\alpha24^+6B11^+CD4^+CD8\beta^-$ cells were sorted using a flow cytometer. The sorted cells were then re-stimulated with irradiated PBMCs pulsed with α-GalCer in the presence of recombinant human IL-2 (rhIL-2) and rhIL-15. Establishment and characterization of iPSCs from the iNKT cells were performed as described previously (Nishimura et al., 2013). In brief, iNKT cells were stimulated with irradiated PBMCs pulsed with α-GalCer and transduced with both reprogramming factors (*OCT3/4*, *KLF4*, *SOX2*, and *C-MYC*) using SeVdp (KOSM) 302L and SV40 large T antigen using SeV18 + SV40LTA/TS15ΔF. Finally, the cells were cultured for several weeks after removal of the SeV vectors from the cytoplasm (Nishimura et al., 2011). The entire study was conducted in accordance with the Declaration of Helsinki and with the approval of institutional ethics boards.

iNKT Cell Differentiation from iNKT-iPSCs

To differentiate iNKT-iPSCs into iNKT cells, we used a previously described T cell differentiation method with slight modification (Nishimura et al., 2013). In brief, clumps of iPSCs were transferred onto C3H10T1/2 feeder cells and cultured in EB medium containing rhVEGF (vascular endothelial growth factor). On day 7, rhSCF and rhFlt3L were added to the culture. On day 14, hematopoietic progenitor cells were collected and transferred onto OP9-DL1 cells and co-cultured in OP9 medium in the presence of rhIL-7 and rhFlt3L. On day 29, rhIL-15 and rhIL-2 were added to the culture (Figure 1B).

Flow Cytometry-Based Assays

Information about the mAbs used for flow cytometry and functional assays are listed in Table S2. Stained cell samples were

analyzed using a FACSCalibur or FACSAriaII flow cytometer (BD Biosciences), and the data were processed using FlowJo (Tree Star). CD1d-tetramer (Proimmune) and HLA-A*24:02/WT1$_{235–243}$ tetramer were used to detect iNKT cells and WT1 peptide-specific CTLs, respectively, with HLA-A*24:02/HIV Env$_{584–592}$ tetramer serving as a negative control. Relative telomere length was measured with a telomere PNA kit/fluorescein isothiocyanate (DAKO). Levels of human cytokines in the culture supernatants were evaluated using a bead-based multiplex immunoassay (FlowCytomix; Affymetrix eBiosciences and BD Cytometric Beads Array; BD Biosciences) or ELISA (Affymetrix eBiosciences). For the multiplex assay, data were acquired on a FACSCanto flow cytometer (BD Biosciences).

Cell Proliferation

Cell proliferation was evaluated by direct enumeration of cells and by using [^{3}H]thymidine incorporation assays as described by Liu et al. (2008).

CTL Priming and Cytotoxicity Assays

Both parental iNKT cells and re-differentiated iNKT cells were stimulated with irradiated PBMCs pulsed with α-GalCer in the presence of rhIL-2 and rhIL-15. Vehicle- or α-GalCer-pulsed autologous DCs were cultured with the cells for 12 hr. The differentially conditioned DCs were then irradiated and cultured with CD8$^+$ T cells in the presence of WT1$_{235–243}$ peptide. After 6 days of culture, the proliferative responses of the cells were measured by [^{3}H] thymidine incorporation assay. After 10 days of culture, the frequencies of WT1 peptide-specific CTLs were determined using HLA-A*24:02/WT1$_{235–243}$ tetramer, and the cells were re-stimulated using irradiated autologous PBMCs pre-pulsed with WT1 peptide in the presence of rhIL-2. After an additional 9 days of culture, the expansion of WT1 peptide-specific CTLs was determined. The cytotoxicity of the CTLs and re-iNKT cells was measured using standard ^{51}Cr-release assays.

RNA Sequencing of Re-iNKT Cells

We extracted total RNA using an RNeasy micro kit (Qiagen) as instructed by the manufacturer. cDNA was synthesized using a SMARTer Ultra Low Input RNA for Illumina Sequencing -HV kit (Clontech), after which the Illumina library was prepared using a Low Input Library Prep kit (Clontech). The libraries were sequenced using HiSeq 2500 in 101 cycle Single-Read mode. All sequence reads were extracted in FASTQ format using BCL2FASTQ Conversion Software 1.8.4 in the CASAVA 1.8.2 pipeline. The sequence reads were mapped to hg19 reference genes, downloaded on December 10, 2012 using TopHat v2.0.8b, and quantified using RPKMforGenes. The data have been deposited in NCBI Gene Expression Omnibus (http://www.ncbi.nlm.nih.gov/geo/) and are accessible through GEO: GSE76371 for gene expression microarray and GEO: GSE76372 for genome-wide DNA methylation analysis.

Statistics

PRISM (GraphPad Software) was used for all statistical analyses. t Tests for paired or unpaired data were used to assess the significance of differences between the means of two experimental groups.

SUPPLEMENTAL INFORMATION

Supplemental Information includes Supplemental Experimental Procedures, six figures, and two tables and can be found with this article online at http://dx.doi.org/10.1016/j.stemcr.2016.01.005.

AUTHOR CONTRIBUTIONS

S. Kitayama and R.Z. performed iPSC establishment and differentiation experiments, and were involved in all analyses; T.Y.L., N.U., S.I., Y.K., Y.Y., M.T., N.H., and T.I. performed parts of the cellular and molecular analyses; A.W. and Y.M. performed gene expression and DNA methylation analysis; M.N. and K.K. provided materials critical for the study; and Y.U. and S. Kaneko were responsible for the overall design of the study and wrote the manuscript.

ACKNOWLEDGMENTS

The authors thank Drs. Shinya Yamanaka, Yasuhiro Yamada, Hiroshi Kawamoto, Yuta Mishima (Kyoto University), and Tetuya Nakatsura (NCC) for helpful discussion; Dr. Ken Nishimura (University of Tsukuba), Ms. Manami Ohtaka (AIST), Kaho Hiramatsu (ACCRI), and Yukiko Kobayashi (Kyoto University) for technical assistance; Dr. Peter Karagiannis (Kyoto University) for editing the manuscript; and Dr. Hiromitsu Nakauchi (The University of Tokyo) for providing the cell lines. This work was supported in part the Japanese Ministry of Education, Culture, Sports, Science and Technology, 23592022 (Y.U.), 26462078 (Y.U.), 25861253 (R.Z.), 26670578 (S. Kaneko), 25114707 "Carcinogenic Spiral"(S. Kaneko), and Core Center for iPS Cell Research of Research Center Network for Realization of Regenerative Medicine (S. Kaneko) by the Japanese Ministry of Education, Culture, Sports, Science and Technology; the Aichi Cancer Research Foundation (Y.U.); Takeda Science Foundation (K.K.), The National Cancer Center Research and Development Fund (25-A-7, Y.U.); Daiwa Securities Health Foundation (Y.U.); Pancreas Research Foundation of Japan (Y.U.); and SENSHIN Medical Research Foundation (Y.U.). S. Kaneko is a founder and shareholder at AsTlym Co., Ltd, and Thyas Co., Ltd. M.N. is a founder and CTO of TOKIWA-Bio Inc.

Received: July 14, 2015
Revised: January 8, 2016
Accepted: January 8, 2016
Published: February 9, 2016

REFERENCES

Berzins, S.P., Smyth, M.J., and Baxter, A.G. (2011). Presumed guilty: natural killer T cell defects and human disease. Nat. Rev. Immunol. *11*, 131–142.

Brennan, P.J., Brigl, M., and Brenner, M.B. (2013). Invariant natural killer T cells: an innate activation scheme linked to diverse effector functions. Nat. Rev. Immunol. *13*, 101–117.

Castillo, E.F., Acero, L.F., Stonier, S.W., Zhou, D., and Schluns, K.S. (2010). Thymic and peripheral microenvironments differentially mediate development and maturation of iNKT cells by IL-15 transpresentation. Blood *116*, 2494–2503.

Cerundolo, V., Silk, J.D., Masri, S.H., and Salio, M. (2009). Harnessing invariant NKT cells in vaccination strategies. Nat. Rev. Immunol. *9*, 28–38.

Chan, C.J., Martinet, L., Gilfillan, S., Souza-Fonseca-Guimaraes, F., Chow, M.T., Town, L., Ritchie, D.S., Colonna, M., Andrews, D.M., and Smyth, M.J. (2014). The receptors CD96 and CD226 oppose each other in the regulation of natural killer cell functions. Nat. Immunol. *15*, 431–438.

Chang, D.H., Osman, K., Connolly, J., Kukreja, A., Krasovsky, J., Pack, M., Hutchinson, A., Geller, M., Liu, N., Annable, R., et al. (2005). Sustained expansion of NKT cells and antigen-specific T cells after injection of alpha-galactosyl-ceramide loaded mature dendritic cells in cancer patients. J. Exp. Med. *201*, 1503–1517.

Cheever, M.A., Allison, J.P., Ferris, A.S., Finn, O.J., Hastings, B.M., Hecht, T.T., Mellman, I., Prindiville, S.A., Viner, J.L., Weiner, L.M., et al. (2009). The prioritization of cancer antigens: a national cancer institute pilot project for the acceleration of translational research. Clin. Cancer Res. *15*, 5323–5337.

De Santo, C., Arscott, R., Booth, S., Karydis, I., Jones, M., Asher, R., Salio, M., Middleton, M., and Cerundolo, V. (2010). Invariant NKT cells modulate the suppressive activity of IL-10-secreting neutrophils differentiated with serum amyloid A. Nat. Immunol. *11*, 1039–1046.

Eberl, G., Di Santo, J.P., and Vivier, E. (2015). The brave new world of innate lymphoid cells. Nat. Immunol. *16*, 1–5.

Godfrey, D.I., and Berzins, S.P. (2007). Control points in NKT-cell development. Nat. Rev. Immunol. *7*, 505–518.

Godfrey, D.I., Stankovic, S., and Baxter, A.G. (2010). Raising the NKT cell family. Nat. Immunol. *11*, 197–206.

Gordy, L.E., Bezbradica, J.S., Flyak, A.I., Spencer, C.T., Dunkle, A., Sun, J., Stanic, A.K., Boothby, M.R., He, Y.W., Zhao, Z., et al. (2011). IL-15 regulates homeostasis and terminal maturation of NKT cells. J. Immunol. *187*, 6335–6345.

Hong, C., Lee, H., Park, Y.K., Shin, J., Jung, S., Kim, H., Hong, S., and Park, S.H. (2009). Regulation of secondary antigen-specific CD8(+) T-cell responses by natural killer T cells. Cancer Res. *69*, 4301–4308.

Johnston, R.J., Comps-Agrar, L., Hackney, J., Yu, X., Huseni, M., Yang, Y., Park, S., Javinal, V., Chiu, H., Irving, B., et al. (2014). The immunoreceptor TIGIT regulates antitumor and antiviral CD8(+) T cell effector function. Cancer Cell *26*, 923–937.

Kuylenstierna, C., Bjorkstrom, N.K., Andersson, S.K., Sahlstrom, P., Bosnjak, L., Paquin-Proulx, D., Malmberg, K.J., Ljunggren, H.G., Moll, M., and Sandberg, J.K. (2011). NKG2D performs two functions in invariant NKT cells: direct TCR-independent activation of NK-like cytolysis and co-stimulation of activation by CD1d. Eur. J. Immunol. *41*, 1913–1923.

Li, P., Burke, S., Wang, J., Chen, X., Ortiz, M., Lee, S.C., Lu, D., Campos, L., Goulding, D., Ng, B.L., et al. (2010). Reprogramming of T cells to natural killer-like cells upon Bcl11b deletion. Science *329*, 85–89.

Liu, T.Y., Uemura, Y., Suzuki, M., Narita, Y., Hirata, S., Ohyama, H., Ishihara, O., and Matsushita, S. (2008). Distinct subsets of human invariant NKT cells differentially regulate T helper responses via dendritic cells. Eur. J. Immunol. *38*, 1012–1023.

Maus, M.V., Fraietta, J.A., Levine, B.L., Kalos, M., Zhao, Y., and June, C.H. (2014). Adoptive immunotherapy for cancer or viruses. Annu. Rev. Immunol. *32*, 189–225.

McEwen-Smith, R.M., Salio, M., and Cerundolo, V. (2015). The Regulatory role of invariant NKT cells in tumor immunity. Cancer Immunol. Res. *3*, 425–435.

Metelitsa, L.S., Weinberg, K.I., Emanuel, P.D., and Seeger, R.C. (2003). Expression of CD1d by myelomonocytic leukemias provides a target for cytotoxic NKT cells. Leukemia *17*, 1068–1077.

Mittal, D., Gubin, M.M., Schreiber, R.D., and Smyth, M.J. (2014). New insights into cancer immunoediting and its three component phases—elimination, equilibrium and escape. Curr. Opin. Immunol. *27*, 16–25.

Molling, J.W., Kolgen, W., van der Vliet, H.J., Boomsma, M.F., Kruizenga, H., Smorenburg, C.H., Molenkamp, B.G., Langendijk, J.A., Leemans, C.R., von Blomberg, B.M., et al. (2005). Peripheral blood IFN-gamma-secreting Valpha24+Vbeta11+ NKT cell numbers are decreased in cancer patients independent of tumor type or tumor load. Int. J. Cancer *116*, 87–93.

Molling, J.W., Langius, J.A., Langendijk, J.A., Leemans, C.R., Bontkes, H.J., van der Vliet, H.J., von Blomberg, B.M., Scheper, R.J., and van den Eertwegh, A.J. (2007). Low levels of circulating invariant natural killer T cells predict poor clinical outcome in patients with head and neck squamous cell carcinoma. J. Clin. Oncol. *25*, 862–868.

Motohashi, S., Ishikawa, A., Ishikawa, E., Otsuji, M., Iizasa, T., Hanaoka, H., Shimizu, N., Horiguchi, S., Okamoto, Y., Fujii, S., et al. (2006). A phase I study of in vitro expanded natural killer T cells in patients with advanced and recurrent non-small cell lung cancer. Clin. Cancer Res. *12*, 6079–6086.

Motohashi, S., Nagato, K., Kunii, N., Yamamoto, H., Yamasaki, K., Okita, K., Hanaoka, H., Shimizu, N., Suzuki, M., Yoshino, I., et al. (2009). A phase I-II study of alpha-galactosylceramide-pulsed IL-2/GM-CSF-cultured peripheral blood mononuclear cells in patients with advanced and recurrent non-small cell lung cancer. J. Immunol. *182*, 2492–2501.

Motz, G.T., and Coukos, G. (2013). Deciphering and reversing tumor immune suppression. Immunity *39*, 61–73.

Nicol, A., Nieda, M., Koezuka, Y., Porcelli, S., Suzuki, K., Tadokoro, K., Durrant, S., and Juji, T. (2000). Human invariant valpha24+ natural killer T cells activated by alpha-galactosylceramide (KRN7000) have cytotoxic anti-tumour activity through mechanisms distinct from T cells and natural killer cells. Immunology *99*, 229–234.

Nicol, A.J., Tazbirkova, A., and Nieda, M. (2011). Comparison of clinical and immunological effects of intravenous and intradermal administration of alpha-galactosylceramide (KRN7000)-pulsed dendritic cells. Clin. Cancer Res. *17*, 5140–5151.

Nieda, M., Nicol, A., Koezuka, Y., Kikuchi, A., Lapteva, N., Tanaka, Y., Tokunaga, K., Suzuki, K., Kayagaki, N., Yagita, H., et al. (2001). TRAIL expression by activated human CD4(+)V alpha 24NKT cells induces in vitro and in vivo apoptosis of human acute myeloid leukemia cells. Blood *97*, 2067–2074.

Nishimura, K., Sano, M., Ohtaka, M., Furuta, B., Umemura, Y., Nakajima, Y., Ikehara, Y., Kobayashi, T., Segawa, H., Takayasu, S., et al. (2011). Development of defective and persistent Sendai virus

vector: a unique gene delivery/expression system ideal for cell reprogramming. J. Biol. Chem. *286*, 4760–4771.

Nishimura, T., Kaneko, S., Kawana-Tachikawa, A., Tajima, Y., Goto, H., Zhu, D., Nakayama-Hosoya, K., Iriguchi, S., Uemura, Y., Shimizu, T., et al. (2013). Generation of rejuvenated antigen-specific T cells by reprogramming to pluripotency and redifferentiation. Cell Stem Cell *12*, 114–126.

Noy, R., and Pollard, J.W. (2014). Tumor-associated macrophages: from mechanisms to therapy. Immunity *41*, 49–61.

Postow, M.A., Callahan, M.K., and Wolchok, J.D. (2015). Immune checkpoint blockade in cancer therapy. J. Clin. Oncol. *33*, 1974–1982.

Richter, J., Neparidze, N., Zhang, L., Nair, S., Monesmith, T., Sundaram, R., Miesowicz, F., Dhodapkar, K.M., and Dhodapkar, M.V. (2013). Clinical regressions and broad immune activation following combination therapy targeting human NKT cells in myeloma. Blood *121*, 423–430.

Salio, M., Silk, J.D., Jones, E.Y., and Cerundolo, V. (2014). Biology of CD1- and MR1-restricted T cells. Annu. Rev. Immunol. *32*, 323–366.

Schietinger, A., and Greenberg, P.D. (2014). Tolerance and exhaustion: defining mechanisms of T cell dysfunction. Trends Immunol. *35*, 51–60.

Schreiber, R.D., Old, L.J., and Smyth, M.J. (2011). Cancer immunoediting: integrating immunity's roles in cancer suppression and promotion. Science *331*, 1565–1570.

Shah, D.K., and Zuniga-Pflucker, J.C. (2014). An overview of the intrathymic intricacies of T cell development. J. Immunol. *192*, 4017–4023.

Song, L., Asgharzadeh, S., Salo, J., Engell, K., Wu, H.W., Sposto, R., Ara, T., Silverman, A.M., DeClerck, Y.A., Seeger, R.C., et al. (2009). Valpha24-invariant NKT cells mediate antitumor activity via killing of tumor-associated macrophages. J. Clin. Invest. *119*, 1524–1536.

Stanietsky, N., Simic, H., Arapovic, J., Toporik, A., Levy, O., Novik, A., Levine, Z., Beiman, M., Dassa, L., Achdout, H., et al. (2009). The interaction of TIGIT with PVR and PVRL2 inhibits human NK cell cytotoxicity. Proc. Natl. Acad. Sci. USA *106*, 17858–17863.

Takahashi, T., Nieda, M., Koezuka, Y., Nicol, A., Porcelli, S.A., Ishikawa, Y., Tadokoro, K., Hirai, H., and Juji, T. (2000). Analysis of human V alpha 24+ CD4+ NKT cells activated by alpha-glycosylceramide-pulsed monocyte-derived dendritic cells. J. Immunol. *164*, 4458–4464.

Trinchieri, G. (2003). Interleukin-12 and the regulation of innate resistance and adaptive immunity. Nat. Rev. Immunol. *3*, 133–146.

Uchida, T., Horiguchi, S., Tanaka, Y., Yamamoto, H., Kunii, N., Motohashi, S., Taniguchi, M., Nakayama, T., and Okamoto, Y. (2008). Phase I study of alpha-galactosylceramide-pulsed antigen presenting cells administration to the nasal submucosa in unresectable or recurrent head and neck cancer. Cancer Immunol. Immunother. *57*, 337–345.

Uemura, Y., Liu, T.Y., Narita, Y., Suzuki, M., Nakatsuka, R., Araki, T., Matsumoto, M., Iwai, L.K., Hirosawa, N., Matsuoka, Y., et al. (2009). Cytokine-dependent modification of IL-12p70 and IL-23 balance in dendritic cells by ligand activation of Valpha24 invariant NKT cells. J. Immunol. *183*, 201–208.

Veillette, A., Dong, Z., and Latour, S. (2007). Consequence of the SLAM-SAP signaling pathway in innate-like and conventional lymphocytes. Immunity *27*, 698–710.

Vizcardo, R., Masuda, K., Yamada, D., Ikawa, T., Shimizu, K., Fujii, S., Koseki, H., and Kawamoto, H. (2013). Regeneration of human tumor antigen-specific T cells from iPSCs derived from mature CD8(+) T cells. Cell Stem Cell *12*, 31–36.

Watarai, H., Fujii, S., Yamada, D., Rybouchkin, A., Sakata, S., Nagata, Y., Iida-Kobayashi, M., Sekine-Kondo, E., Shimizu, K., Shozaki, Y., et al. (2010). Murine induced pluripotent stem cells can be derived from and differentiate into natural killer T cells. J. Clin. Invest. *120*, 2610–2618.

Yamasaki, K., Horiguchi, S., Kurosaki, M., Kunii, N., Nagato, K., Hanaoka, H., Shimizu, N., Ueno, N., Yamamoto, S., Taniguchi, M., et al. (2011). Induction of NKT cell-specific immune responses in cancer tissues after NKT cell-targeted adoptive immunotherapy. Clin. Immunol. *138*, 255–265.

Yu, X., Harden, K., Gonzalez, L.C., Francesco, M., Chiang, E., Irving, B., Tom, I., Ivelja, S., Refino, C.J., Clark, H., et al. (2009). The surface protein TIGIT suppresses T cell activation by promoting the generation of mature immunoregulatory dendritic cells. Nat. Immunol. *10*, 48–57.

Stem Cell Reports, Volume *6*

Supplemental Information

Cellular Adjuvant Properties, Direct Cytotoxicity of Re-differentiated Vα24 Invariant NKT-like Cells from Human Induced Pluripotent Stem Cells

Shuichi Kitayama, Rong Zhang, Tian-Yi Liu, Norihiro Ueda, Shoichi Iriguchi, Yutaka Yasui, Yohei Kawai, Minako Tatsumi, Norihito Hirai, Yasutaka Mizoro, Tatsuaki Iwama, Akira Watanabe, Mahito Nakanishi, Kiyotaka Kuzushima, Yasushi Uemura, and Shin Kaneko

Figure S1

A

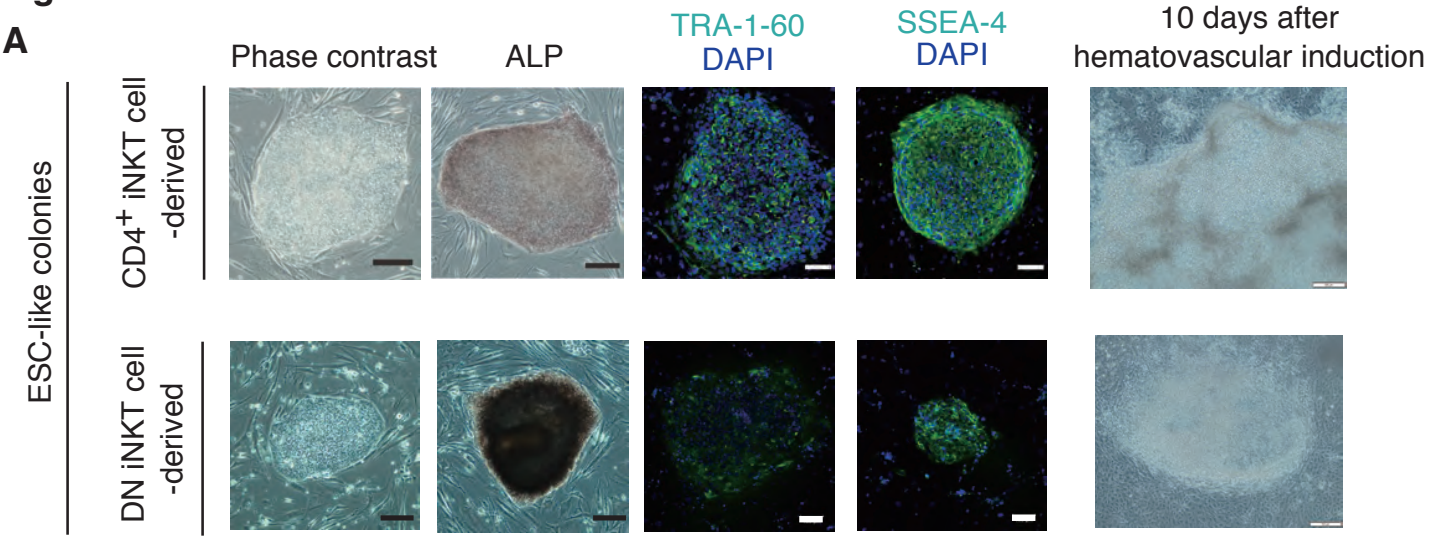

B

Cell source	Donor	Initial cell number ($\times 10^6$)	No. of ESC-like colonies observed at day 21 of induction	No. of transgene-free colonies / No. of colonies picked-up
CD4+ iNKT	A	1.0	82	5 / 5 (100%)
	A	0.5	47	
CD4+ iNKT	B	1.0	>100	6 / 7 (86%)
	B	0.5	>100	
DN iNKT	B	>1.0	38	0 / 6 (0%)
DN iNKT	C	>1.0	63	0 / 24 (0%)

C

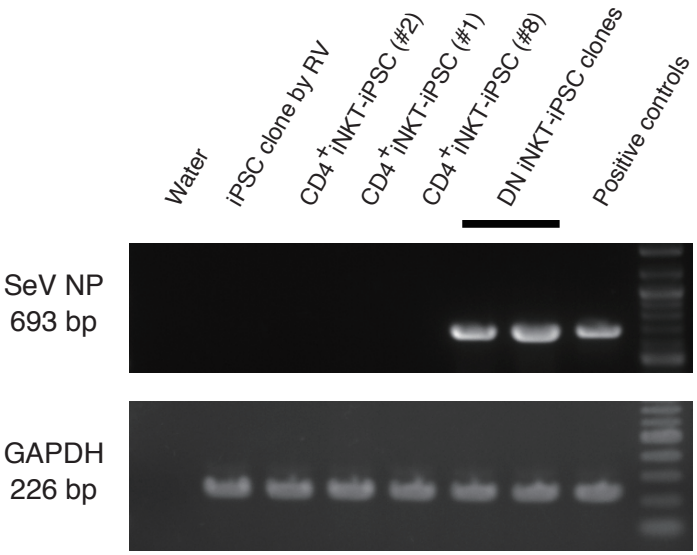

D

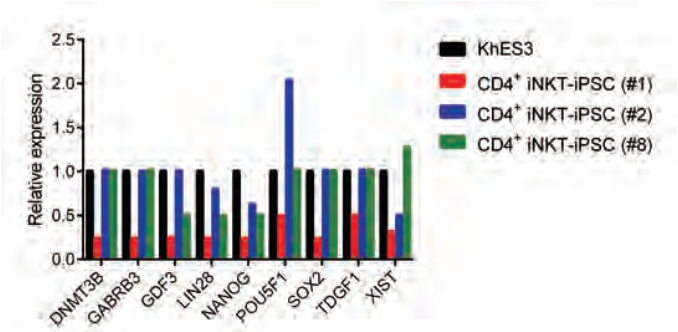

E

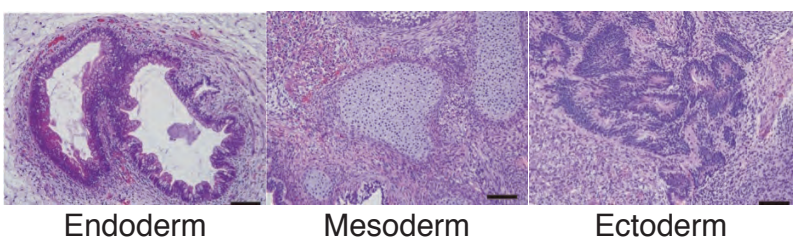

F

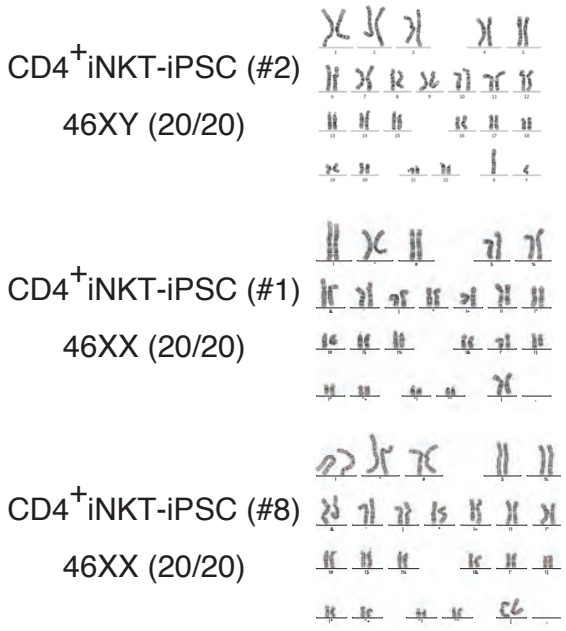

Figure S2

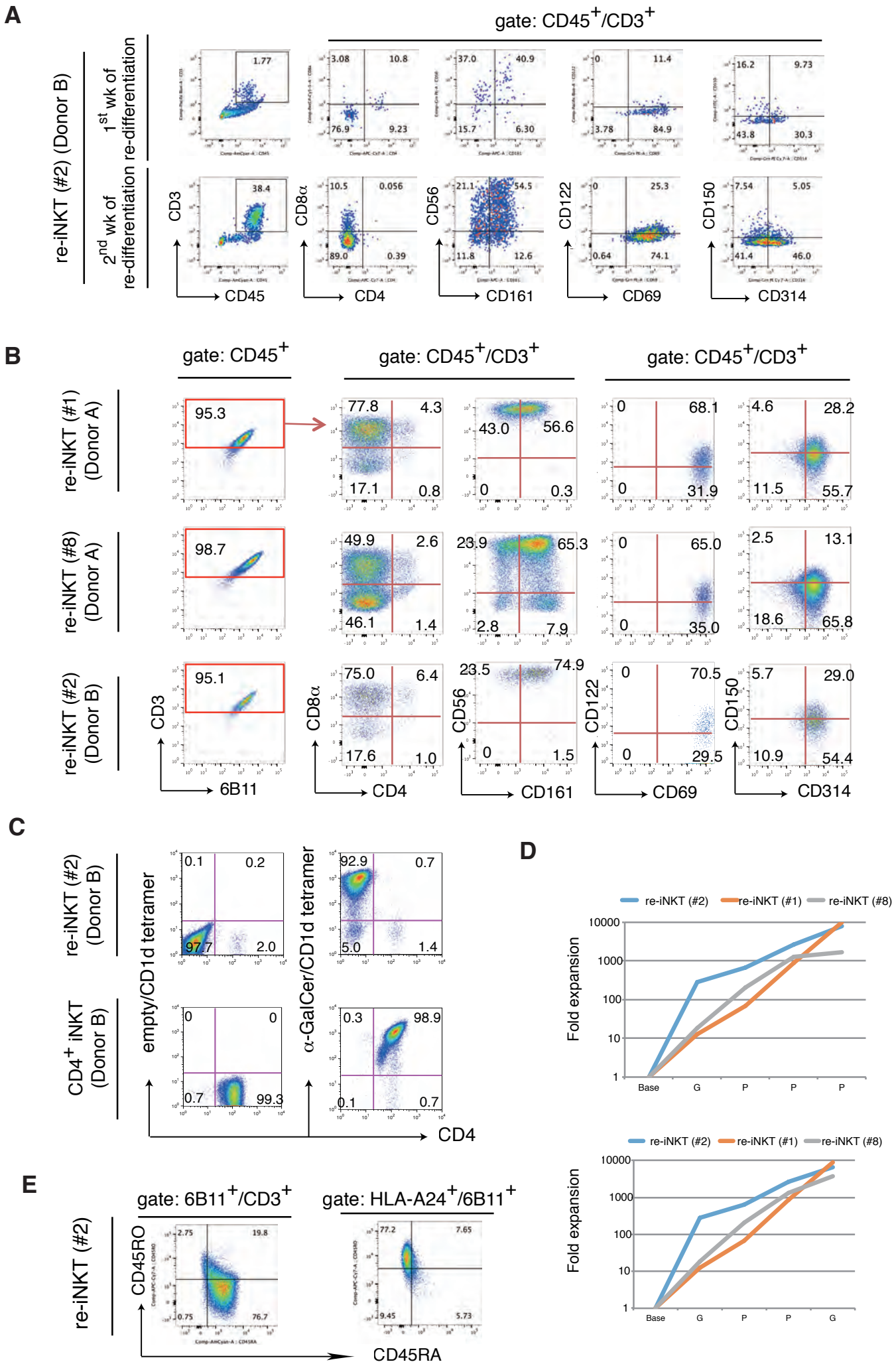
A
gate: CD45+/CD3+
re-iNKT (#2) (Donor B)
1st wk of re-differentiation
2nd wk of re-differentiation
CD3
CD45
CD8α
CD4
CD56
CD161
CD122
CD69
CD150
CD314
B
gate: CD45+
gate: CD45+/CD3+
re-iNKT (#1) (Donor A)
re-iNKT (#8) (Donor A)
re-iNKT (#2) (Donor B)
6B11
C
CD4+ iNKT (Donor B)
empty/CD1d tetramer
α-GalCer/CD1d tetramer
D
re-iNKT (#2)
re-iNKT (#1)
re-iNKT (#8)
Fold expansion
Base
G
P
E
gate: 6B11+/CD3+
gate: HLA-A24+/6B11+
CD45RO
CD45RA

Figure S3

A

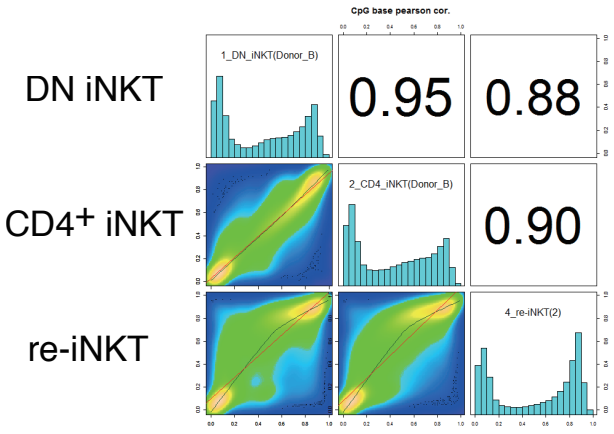
CpG base pearson cor.
DN iNKT
CD4+ iNKT
re-iNKT
1_DN_iNKT(Donor_B)
2_CD4_iNKT(Donor_B)
4_re-iNKT(2)
0.95
0.88
0.90

B

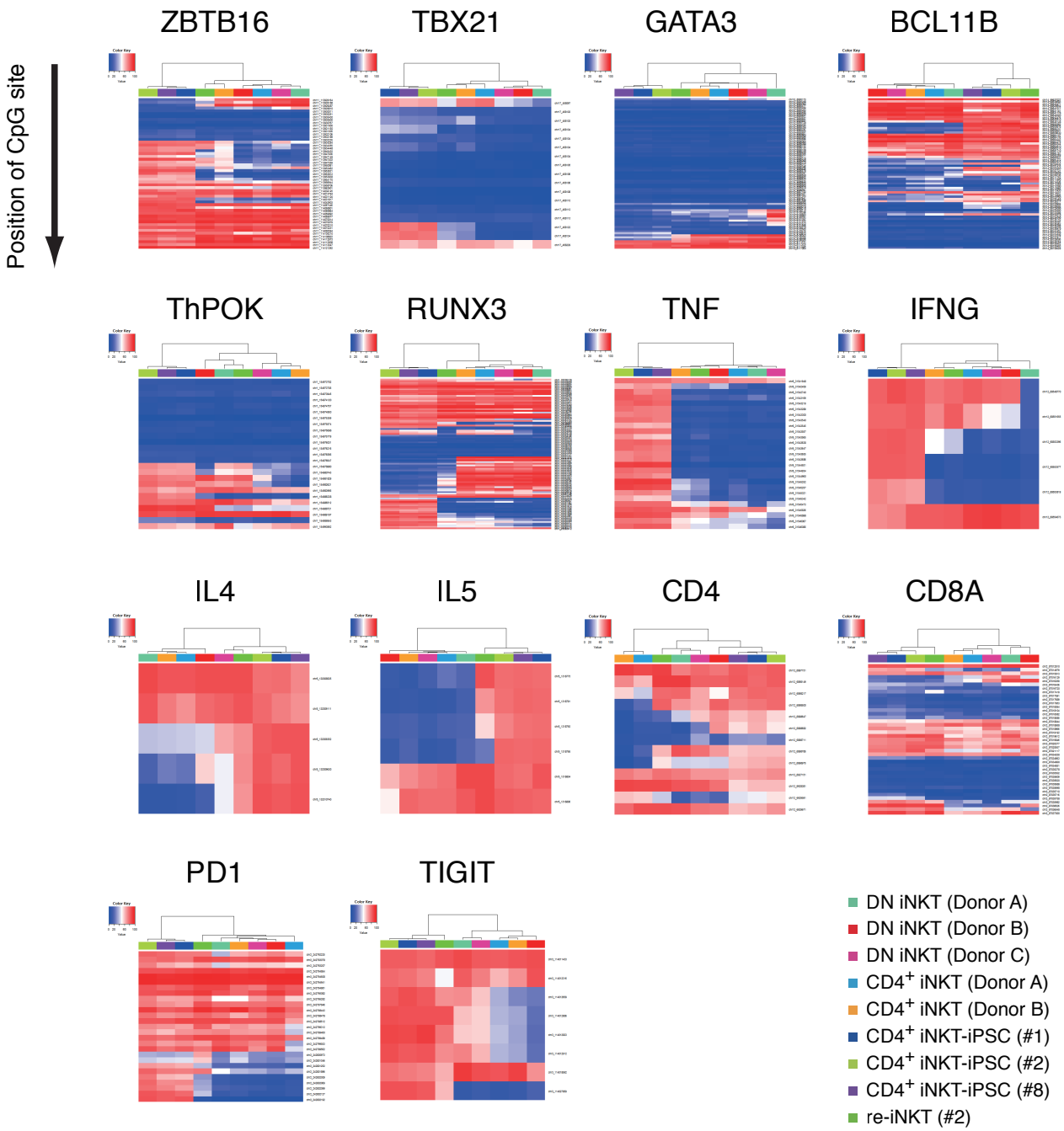
ZBTB16
TBX21
GATA3
BCL11B
Position of CpG site
ThPOK
RUNX3
TNF
IFNG
IL4
IL5
CD4
CD8A
PD1
TIGIT
DN iNKT (Donor A)
DN iNKT (Donor B)
DN iNKT (Donor C)
CD4+ iNKT (Donor A)
CD4+ iNKT (Donor B)
CD4+ iNKT-iPSC (#1)
CD4+ iNKT-iPSC (#2)
CD4+ iNKT-iPSC (#8)
re-iNKT (#2)

Figure S4

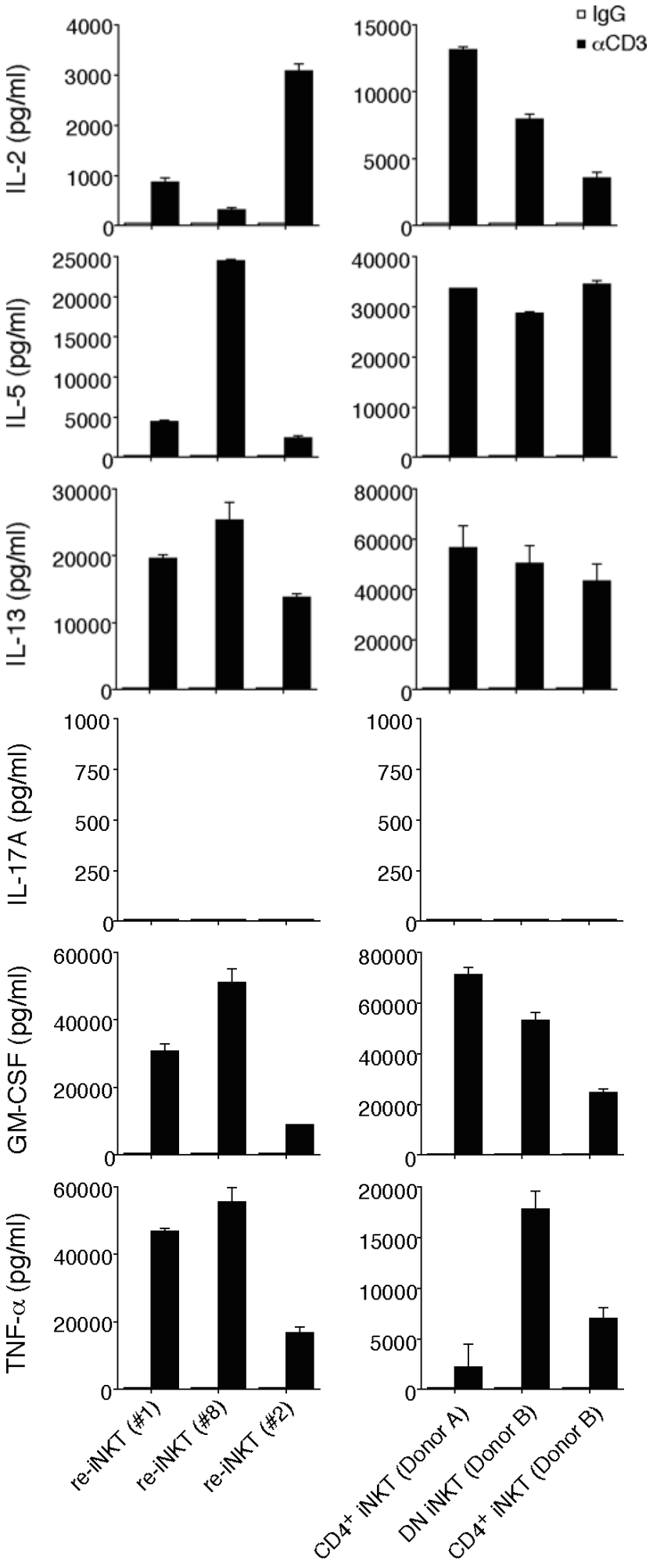
IgG
αCD3
IL-2 (pg/ml)
IL-5 (pg/ml)
IL-13 (pg/ml)
IL-17A (pg/ml)
GM-CSF (pg/ml)
TNF-α (pg/ml)
re-iNKT (#1)
re-iNKT (#8)
re-iNKT (#2)
CD4+ iNKT (Donor A)
DN iNKT (Donor B)
CD4+ iNKT (Donor B)

Figure S5

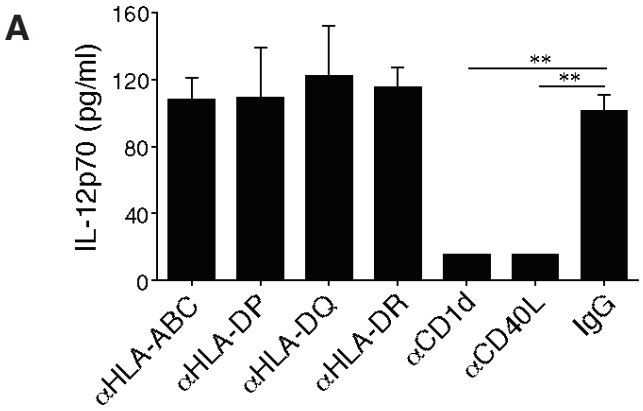
A
IL-12p70 (pg/ml)
160
120
80
40
0
**
**
αHLA-ABC
αHLA-DP
αHLA-DQ
αHLA-DR
αCD1d
αCD40L
IgG

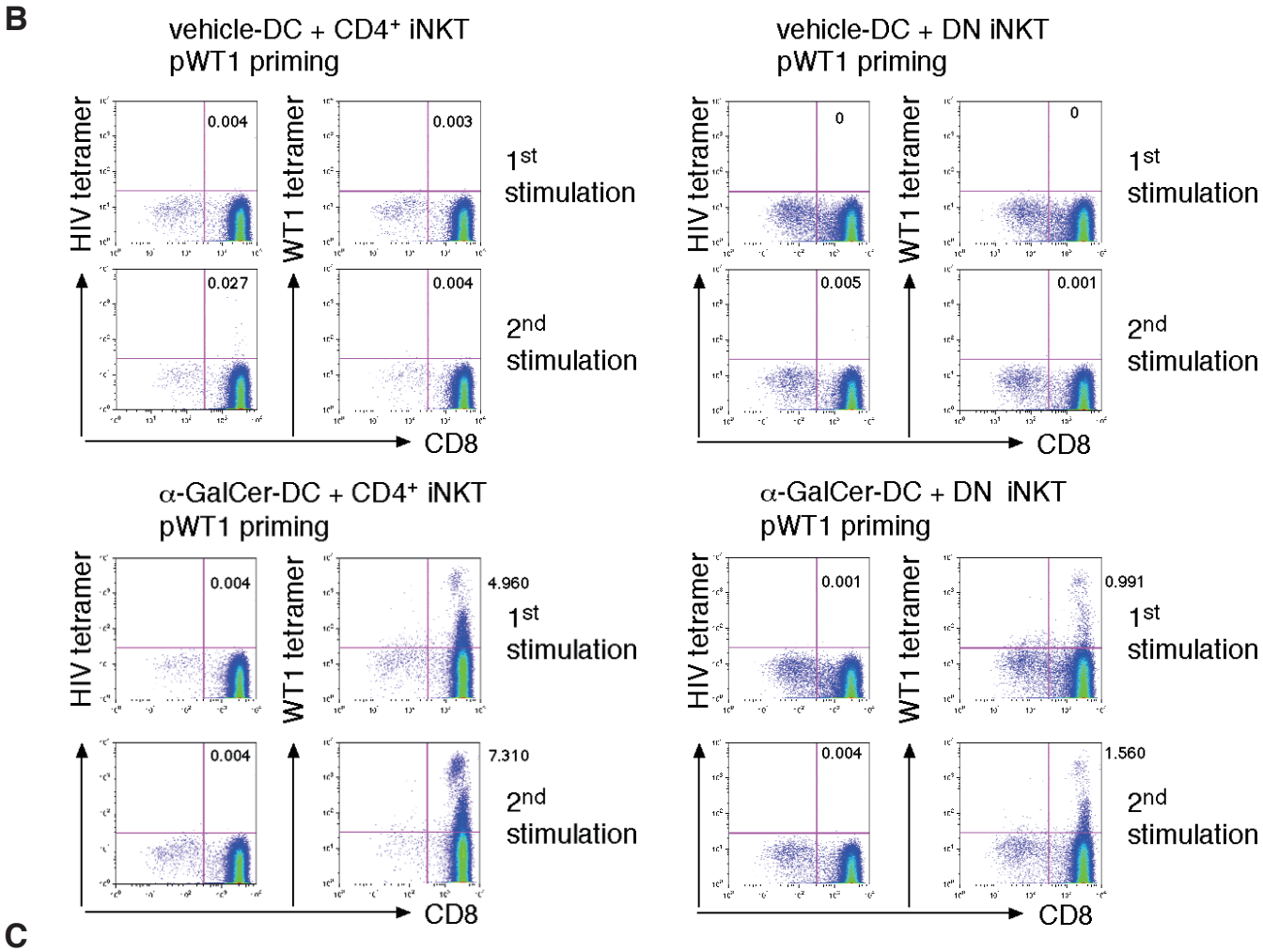
B
vehicle-DC + CD4+ iNKT
pWT1 priming
vehicle-DC + DN iNKT
pWT1 priming
HIV tetramer
WT1 tetramer
0.004
0.003
0.027
0.004
0
0
0.005
0.001
1st stimulation
2nd stimulation
CD8
α-GalCer-DC + CD4+ iNKT
pWT1 priming
α-GalCer-DC + DN iNKT
pWT1 priming
0.004
4.960
0.004
7.310
0.001
0.991
0.004
1.560

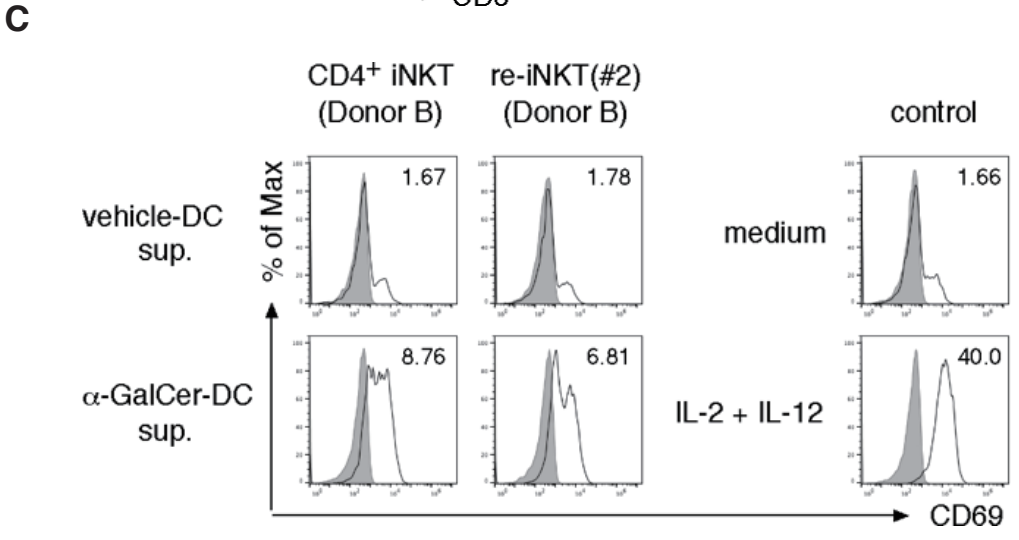
C
CD4+ iNKT
(Donor B)
re-iNKT(#2)
(Donor B)
control
vehicle-DC
sup.
α-GalCer-DC
sup.
% of Max
1.67
1.78
1.66
8.76
6.81
40.0
medium
IL-2 + IL-12
CD69

Figure S6

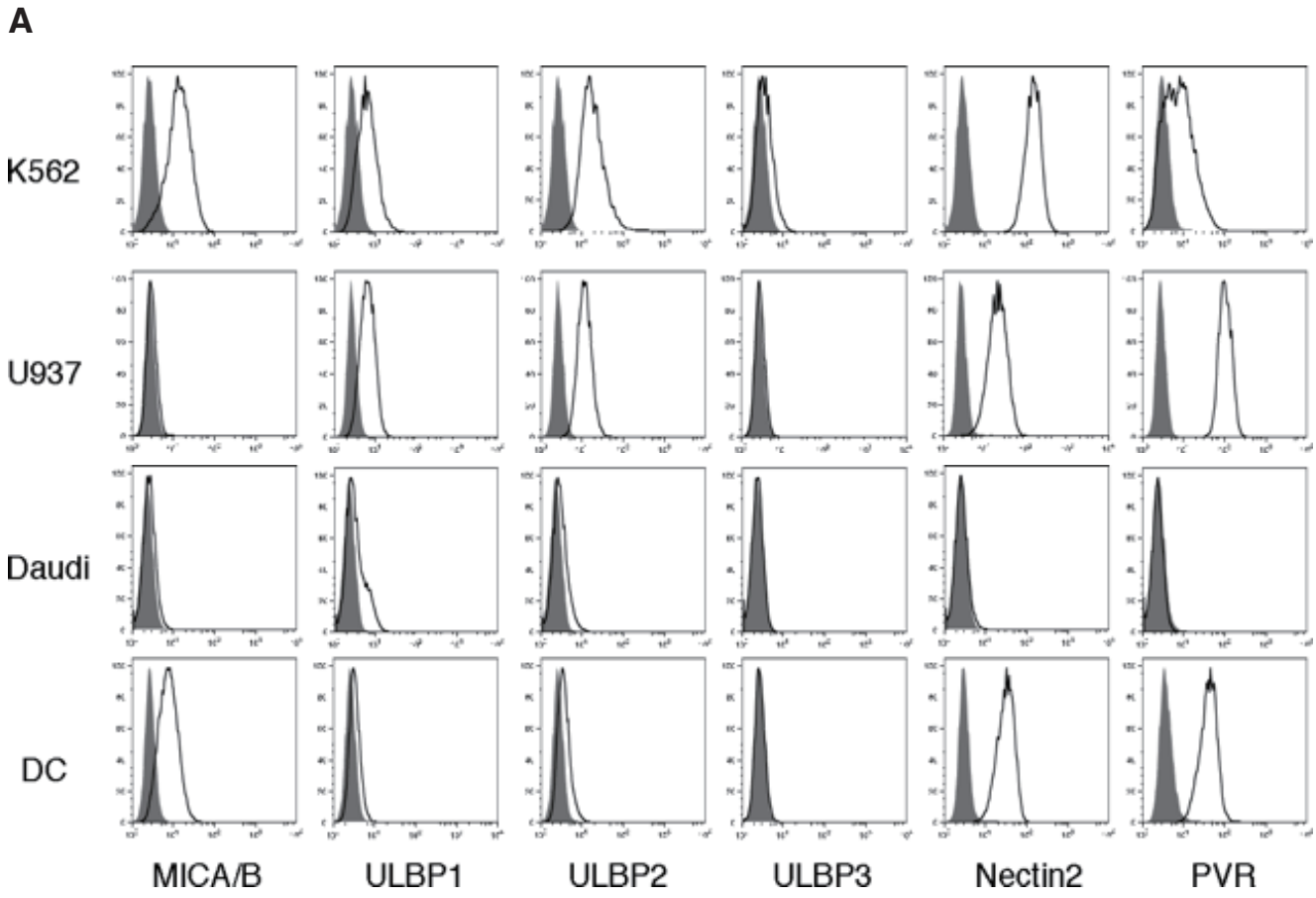
A
K562
U937
Daudi
DC
MICA/B
ULBP1
ULBP2
ULBP3
Nectin2
PVR

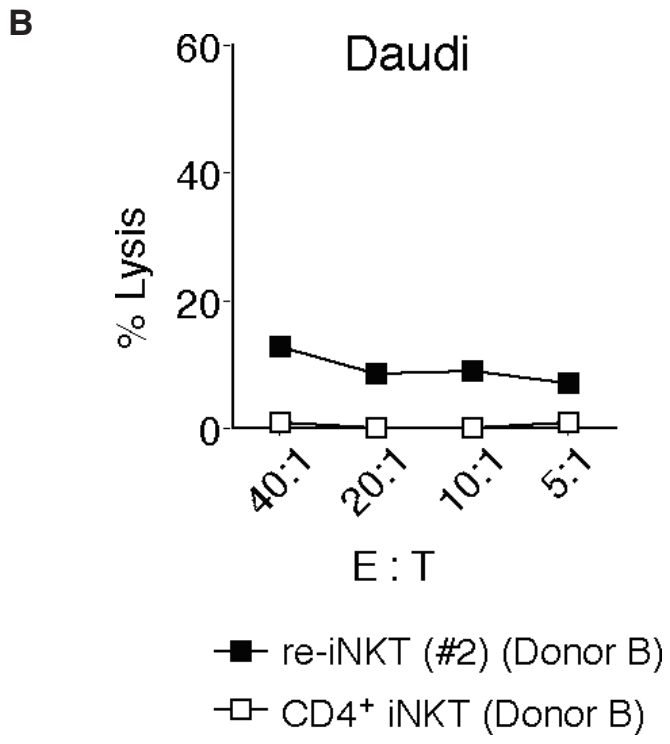
B
Daudi
% Lysis
60
40
20
0
40:1
20:1
10:1
5:1
E : T
re-iNKT (#2) (Donor B)
CD4+ iNKT (Donor B)

Supplemental Information

Supplemental Figure Legends

Figure S1

Generation of iPSCs from human CD4$^+$ iNKT cells

(A) CD4$^+$ and DN iNKT cell-derived ESC-like colonies and sac-like hematopoietic structures derived from the colonies. Shown are phase contrast, alkaline phosphatase stained and immunofluorescent images of representative iNKT cell-derived ESC-like colonies. The upper right image shows hematopoietic cells in a sac-like structure observed in a differentiation culture of CD4$^+$ iNKT-iPSCs. In contrast, no hematopoietic cells were observed in a differentiation culture from DN iNKT-iPSCs. Scale bar = 100 μm. (B) Numbers of ESC-like colonies derived from CD4$^+$ or DN iNKT cells from multiple donors. (C) PCR-based analysis for detection of Sendai virus genomic RNA remnants. No established CD4$^+$ iNKT-iPSC colonies retained remnant Sendai virus. SeV NP, sendai virus vector nucreocapside protein; RV, retroviral vector. (D) Quantitative PCR analysis for the indicated pluripotency-related genes in the indicated human embryonic cell lines. Individual PCR reactions were normalized to 18S ribosomal RNA (rRNA). Relative expression values to embryonic stem cell line KhES3 are indicated. Data was run in triplicate in 2 independent experiments. (E) Representative HE-stained sections of a CD4$^+$ iNKT-iPSC (clone #2)-derived teratoma from a NOD/ShiJic-scid mouse. The iPSCs differentiated into cell lineages derived from endoderm, mesoderm and ectoderm. (F) Karyotype analysis of CD4$^+$ iNKT-iPSCs clones #1 , #2 and #8.

Figure S2, Related to Figure 1:

Phenotypic profile and proliferative potential of re-iNKT cells

(A) Flow cytometric analysis of cells from $CD4^+$ iNKT-iPSC clone #2 on 1^{st} and 2^{nd} week of re-differentiation on OP9/DL1. Shown are the surface protein expression patterns on re-differentiating cells from a representative experiment. (B) Flow cytometric analysis of cells re-differentiating from $CD4^+$ iNKT-iPSC clones #1, #2 and #8 35 days after inducing re-differentiation. Shown are the surface protein expression patterns on re-differentiating cells gated by CD45, CD3 and 6B11. The results are representative of more than 5 independent experiments from the 3 clones and control PBMCs. (C) α-GalCer/CD1d tetramer staining. Re-iNKT cells #2 (upper panels) or parental iNKT cells (lower panels) were stained with negative control CD1d tetramer (left panels) or α-GalCer-loaded CD1d tetramer (right panels) followed by anti-CD4 mAb. (D) Stimulation-mediated expansion of re-iNKT cells. Re-iNKT cells were initially stimulated with α-GalCer-pulsed PBMCs then expanded by PHA-P or α-GalCer-pulsed PBMCs. Shown are representative results from re-iNKT cells derived from the 3 clones. G: α-GalCer, P: PHA-P. (E) Expression profile of CD45RA and CD45RO before (left panel) and after (right panel) α-GalCer stimulation on re-iNKT cells (clone #2).

Figure S3, Related to Figure 2:

DNA methylation profiles of re-iNKT cells

(A) Density plots of DNA methylation levels for DN iNKT (Donor B) vs. $CD4^+$ iNKT (Donor B) (top), DN iNKT (Donor B) vs. re-iNKT (middle), and $CD4^+$ iNKT (Donor B) vs. re-iNKT (botom). Numbers in the panels denote pair-wise Pearson's correlation scores. The histograms on the diagonal describe distributions of CpGs with different DNA methylation levels.

(B) Differential regulation of DNA methylation on differentiation- and function-related genes. Heatmaps visualize DNA methylation levels for each CpG nucleotide (blue, non-methylated; red, methylated). Unsupervised hierarchical clustering of cell samples was performed using the Euclidian distance and Ward's method.

Figure S4, Related to Figure 3:

Cytokine profiles of re-iNKT cells

Re-iNKT cells (2×10^5 cells/well) were stimulated for 24 h with plate-bound control IgG or anti-CD3 mAb (10 μg/ml), after which the levels of the indicated cytokines in the culture supernatant were evaluated using beads-based multiplex immunoassays (left panels). Responses of parental iNKT cells served as references (right panels). Data were run in triplicate, and the experiment was repeated 2 times. The results of 1 representative experiment are shown. Bars depict means ± s.d.

Figure S5, Related to Figure 4:

Induction of tumor Ag-specific CTLs and NK cells via parental iNKT cell-DC interaction

(A) IL-12p70 production by α-GalCer-DCs stimulated by re-iNKT cells in the presence of blocking antibodies. Data were run in triplicate, and experiments were repeated 2 times; the results of 1 representative experiment are shown. Bars depict means ± s.d. (B) α-GalCer-DCs were cultured for 12 h with $CD4^+$ or DN iNKT cells, irradiated and cultured with autologous $CD8^+$ T cells in the presence of $WT1_{235\text{-}243}$ peptide. After 10 days of culture, the frequencies of $WT1_{235\text{-}243}$-specific CTLs were determined by staining for WT1 tetramer (1st stimulation). The cells were then restimulated by irradiated autologous PBMCs pre-pulsed with $WT1_{235\text{-}243}$ peptide.

After an additional 9 days of culture, the frequencies of $WT1_{235-243}$-specific CTLs were determined by staining for WT1 tetramer (2nd stimulation). HIV tetramer served as a negative control. One representative result from at least 2 independent experiments is shown. WT1 peptide-loaded $CD4^+$ and DN iNKT/α-GalCer-DCs induced expansion of WT1-tetramer-positive T cells more efficiently than WT1 peptide-loaded $CD4^+$ and DN iNKT/vehicle-DCs. The cellular adjuvant properties of $CD4^+$ iNKT cells for antigen-specific CTL priming were superior to those of DN iNKT cells. (C) Representative flow cytometry profiles of surface CD69 on $CD3^+CD56^+$ NK cells cultured for 48 h in the presence of 25% cell-free supernatant taken from iNKT-DC coculture. Medium control and IL-2 (300 IU/ml) plus IL-12 (20 ng/ml) control served as references. Open histograms represent staining for CD69; gray histograms represent isotype control.

Figure S6, Related to Figure 5:

Expression of NKG2D ligands and DNAM-1 ligands in leukemic cell lines and DCs

(A) Surface expression of MICA/B, ULBP1, ULBP2 and ULBP3 as NKG2D ligands, and Nectin2 and PVR as DNAM-1 ligands on K562, U937, Daudi and DCs. Shown are representative staining histograms for the indicated surface molecules (open histograms) and isotype-matched controls (filled histograms). (B) Cytotoxicity toward Daudi cells at the indicated E/T ratios. Daudi cells that expressed neither NKG2D ligand nor DNAM-1 ligands had little susceptibility to re-iNKT cell-lysis.

Table S1. The list of genes extracted for Figure 2C

Gene	Accession
ZBTB16	NM_006006+NM_001018011
TBX21	NM_013351
GATA3	NM_002051+NM_001002295
CCDC22+FOXP3	NM_014008+NM_001114377+NM_014009
RORC	NM_005060+NM_001001523
ZBTB7B(ThPOK)	NR_045515+NM_001252406+NR_049765+NM_001256455+NR_046206
RUNX3	NM_004350+NM_001031680
RUNX1	NM_001754+NM_001001890+NM_001122607
BCL11B	NM_138576+NM_022898
TCF7	NM_003202+NM_001134851+NM_201634+NM_201632+NM_213648+NR_033449
ID3	NM_002167
ID2	NM_002166
ETS1	NM_005238+NM_001143820+NM_001162422
ETS2	NM_001256295+NM_005239
LEF1+LEF1-AS1	NM_001130713+NM_001130714+NM_016269+NM_001166119+NR_029374+NR_029373
HES1	NM_005524
SOX13	NM_005686
MYB	NM_001161660+NM_001161656+NM_001130172+NM_001130173+NM_005375+NM_001161658+NM_001161659+NM_001161657
GFI1	NM_001127216+NM_005263+NM_001127215
TAL1	NM_003189
IKZF1	NM_001220767+NM_001220769+NM_001220768+NM_001220766+NM_001220765+NM_001220774+NM_001220773+NM_001220772+NM_001220771+NM_001220770+NM_006060+NM_001220776+NM_001220775
IKZF2	NM_016260+NM_001079526
IKZF3	NM_183232+NM_012481+NM_001257411+NM_001257410+NM_001257409+NM_183229+NM_183228+NM_001257412+NM_183231+NM_183230+NM_001257408+NM_001257413+NM_001257414+NR_047560+NR_047561+NR_047559
TCF12	NM_207038+NM_207036+NM_003205+NM_207037+NM_207040
GATA2	NM_001145662+NM_001145661+NM_032638
CEBPA	NM_004364
SATB1	NM_001195470+NM_002971+NM_001131010
EOMES	NM_005442
RBPJ	NM_005349+NM_203283+NM_015874+NM_203284
STAT5B	NM_012448
TNF	NM_000594
IFNG	NM_000619
IL2	NM_000586
IL4	NM_000589+NM_172348
IL5	NM_000879
IL10	NM_000572
IL13	NM_002188
IL17A	NM_002190
CSF1	NM_000757+NM_172212+NM_172210+NM_172211
CSF2	NM_000758
IL12RB1	NM_005535+NM_153701
IL12RB2	NM_001559+NR_047584+NM_001258214+NM_001258215+NM_001258216+NR_047583
IL17RB	NM_018725
IL23R	NM_144701
IL4R	NM_000418+NM_001257407+NM_001257997+NM_001257406
CXCR3	NM_001142797+NM_001504
CXCR6	NM_006564
IFNGR1	NM_000416
IL15RA	NM_001256765+NM_002189+NM_172200+NM_001243539+NR_046362
IL2RA	NM_000417
IL2RB	NM_000878
IL2RG	NM_000206
IL7R	NM_002185

Table S2. List of antibodies used in this study

Antigen	Clone	Isotype
CD1d	51.1	mouse IgG2b
CD122	TU27	mouse IgG1
CD150	A12(7D4)	mouse IgG1
CD161	HP-3G10	mouse IgG1
CD183(CXCR3)	G025H7	mouse IgG1
CD196(CCR6)	G034E3	mouse IgG2b
CD226(DNAM-1)	11A-8	mouse IgG1
CD226(DNAM-1)	DX11	mouse IgG1
CD279(PD-1)	EH12.2H7	mouse IgG1
CD3	HIT3a	mouse IgG2a
CD3	UCHT1	mouse IgG1
CD314(NKG2D)	1D11	mouse IgG1
CD4	RPA-T4	mouse IgG1
CD40L	TRAP-1	mouse IgG1
CD40L	40804	mouse IgG2b
CD45	HI30	mouse IgG1
CD56	B159	mouse IgG1
CD56	HCD56	mouse IgG1
CD69	FN50	mouse IgG1
CD86	IT2.2	mouse IgG2b
CD8α	3B5	mouse IgG2a
CD8α	SK1	mouse IgG1
CD96	NK92.39	mouse IgG1
FasL	NOK-1	mouse IgG1
FasL	Polyclonal	goat IgG
granzyme B	GB11	mouse IgG1
HLA-A24	17A10	mouse IgG2b
HLA-ABC	W6/32	mouse IgG2a
HLA-DP	B7/21	mouse IgG3
HLA-DQ	SPVL3	mouse IgG2a
HLA-DR	L243	mouse IgG2a
MIC A/B	6D4	mouse IgG2a
nectin-2	TX31	mouse IgG1
NKp44	p44-8	mouse IgG1
NKp46	9E-2	mouse IgG1
perfolin	dG9	mouse IgG2b
PVR	SKII.4	mouse IgG1
TCR Vα24Jα18	6B11	mouse IgG1
TCR Vβ11	C21	mouse IgG2a
TIGIT	MBSA43	mouse IgG1
TNFα	Polyclonal	goat IgG
TRAILR1	Polyclonal	goat IgG
TRAILR2	B-K29	mouse IgG1
ULBP1	170818	mouse IgG2a
ULBP2	165903	mouse IgG2a
CD16	3G8	mouse IgG1

Isotype control	Clone
mouse IgG1	MOPC-21
mouse IgG1	P3.6.2.8.1
mouse IgG2a	G155-178
mouse IgG2b	eBMG2b

Supplemental Experimental Procedures

Cell lines, peptides, cytokines and chemicals

C1R transfectants were established as described (Liu et al., 2008). The cell lines of myelogenous leukemia K562, histiocytic lymphoma U937 and Burkitt's lymphoma Daudi were purchased. HLA-A*24:02-restricted and modified 9-mer Wilms' tumor gene $(WT1)_{235\text{-}243}$ peptide (CMTWNQMNL) was synthesized by Toray Research Center (Kamakura, Japan). Recombinant human (rh) interleukin (IL)-2, rhIL-4 and rh-granulocyte macrophage colony-stimulating factor (GM-CSF) (Primmune, Kobe, Japan), rhIL-12p70 (R&D systems, Minneapolis, MN, USA), and rhIL-7, rhIL-15 and rh fms-related tyrosine kinase 3 ligand (Flt-3L) (Peprotec, UK) were purchased. rh basic fibroblast growth factor (bFGF) and phytohemagglutinin-P (PHA-P) were purchased from WAKO chemical (Osaka, Japan). Vascular endothelial growth factor (VEGF) and rh stem cell factor (SCF) were purchased from R&D systems. Penicillin-killed *Streptococcus pyogenes* (OK432) was purchased from Chugai Pharmaceutical (Tokyo, Japan). α-galactosylceramide (α-GalCer; KRN7000) was purchased from Funakoshi (Tokyo).

Preparation of human monocyte-derived DCs and $CD8^+$ T cells

Human monocyte-derived-DCs were induced as described previously (Liu et al., 2008). Briefly, $CD14^+$ monocytes were isolated from PBMCs using positive magnetic cell sorting with CD14 microbeads (Miltenyi Biotec, Auburn, CA) and cultured at 1.0×10^6 cells/ml in the presence of rhGM-CSF and rhIL-4 (50 ng/ml each). On day 6, nonadherent DCs were harvested and served as immature DCs. $CD8^+$ T cells were isolated from PBMCs by negative magnetic cell sorting using a $CD8^+$ T cell isolation kit (Miltenyi Biotec).

Preparation and activation of NK cells

PBMCs were stimulated with immobilized anti-CD16 mAb in X-VIVO 20 medium (Lonza, Walkersville, MD) supplemented with 5% heat-inactivated human plasma, rhIL-2, and OK432 for 24 h at 39 °C. Then the cells were harvested and cultured in the presence of rhIL-2 at 37 °C. After 10 days of culture, NK cells were isolated using a NK cell isolation kit (Miltenyi Biotec, Bergisch Gladbach, Germany) and cultured for another 10 days. To acquire the resting state, NK cells were cultured for 24 h in the absence of IL-2. Resting state NK cells were cultured for 48 h in the presence of 25% cell-free supernatant taken from iNKT-DC coculture. To prepare supernatant, vehicle or α-GalCer-DCs (1.0×10^6) were cultured with iNKT cells (5.0×10^5) for 24 h.

RT-PCR and Quantitative PCR

Total RNA was extracted from iPSCs using an RNeasy Micro kit (Qiagen) and reverse transcribed using High Capacity cDNA Reverse Transcription kits (Applied Biosystems) with random 6-mer primers. RT-PCR was performed using ExTaq HS (Takara). Individual PCR reactions were normalized against GAPDH rRNA. Primer sequences used in RT-PCR were, 5'-AGACCCTAAGAGGACGAAGA-3' (forward) and 5'-ACTCCCATGGCGTAACTCCATAGTG-3' (reverse) for SeV NP, 5'-GAAGGTGAAGGTCGGAGTC-3' (forward) and 5'-GAAGATGGTGATGGGATTTC-3' (reverse) for GAPDH. Quantitative-PCR was performed using a TaqMan Array Human Stem Cell Pluripotency Card (Applied Biosystems). Individual PCR reactions were normalized against 18S rRNA.

Immunohistochemistry

Human ESC/iPSC colonies fixed in 4% paraformaldehyde were blocked with 8% goat serum and stained with primary antibodies (anti-SSEA-4 1:50, sc-21704, Santa Cruz; anti-TRA-1-60 1:100, MAB4360, Millipore), after which they were stained with secondary antibody (goat anti-mouse IgG, 1:500, A11029, Invitrogen). Nuclei were counterstained with 4', 6-diamidino-2-phenylindol (DAPI; S-1200, Vector Laboratories) according to the manufacturer's instructions. Photomicrographs were taken with a LSM710 confocal microscope (Carl Zeiss).

Teratoma formation

iNKT-iPSC colonies were trypsinized and injected (1.0×10^6 cells/mouse) into the medulla of the testis of NOD/ShiJic-*scid* mice. Nine to twelve weeks after injection, tumors that formed in the testis were extracted, fixed in formalin and embedded in paraffin.

Karyotype analysis

The iPS cell karyotype was determined by LSI Medience Corporation (Tokyo, JAPAN) using the standard staining protocol for Giemsa-banding.

Microarray-based DNA methylation analysis

The EZ DNA methylation kit (Zymo Research, Irvine, CA) was used for bisulfite conversion of 500 ng genomic DNA. Bisulfite-converted DNA was then hybridized to HumanMethylation450 BeadChip (Illumina, San Diego, CA) following the Illumina Infinium HD Methylation protocol. Fluorescent signals were read by iScan (Illumina) and normalized by GenomeStudio V2011.1 (Illumina). DNA methylation levels were calculated by GenomeStudio and are represented as β-values ranging from 0 (non-methylated) to 1 (completely methylated). β-values with detection

P-value ≥ 0.05 and probes whose annotations were not given in RefSeq were removed. Bioinformatic analysis was conducted using R 3.1.0 including R package methylKit (Akalin A, et al., Genome Biol., 2012). The gene region from 1,500 bp upstream of the transcription start site (TSS) to the 3' end of the coding region was subjected to analysis to identify differentially DNA methylated genes. Heatmap visualization and hierarchical clustering were conducted using the heatmap.2 function in gplots and hclust function in R, respectively.

Reference

Akalin, A., Kormaksson, M., Li, S., Garrett-Bakerman, F.E., Figueroa, M.E., Melnick, A., and Mason, C.E.（2012）. methylKit: a comprehensive R package for the analysis of genome-wide DNA methylation profiles. Genome biology *13*, R87

Liu, T.Y., Uemura, Y., Suzuki, M., Narita, Y., Hirata, S., Ohyama, H., Ishihara, O., and Matsushita, S. (2008). Distinct subsets of human invariant NKT cells differentially regulate T helper responses via dendritic cells. European journal of immunology *38*, 1012-1023.